Research Square

Preprints are preliminary reports that have not undergone peer review.
They should not be considered conclusive, used to inform clinical practice,
or referenced by the media as validated information.

Rapid Cycling-Mediated Indirect Facilitation: A Formal Hypothesis on the Maintenance of Plankton Diversity

Hao Duan

2547313804@qq.com

Independent researcher

Research Article

Keywords: Paradox of the plankton, Competitive exclusion, Niche, Microbial loop, Material cycling, Indirect facilitation, Unified coupled population, Evolutionary stability, Formal hypothesis

Posted Date: November 13th, 2026

DOI: https://doi.org/10.21203/rs.3.rs-11306961/v1

License: This work is licensed under a Creative Commons Attribution 4.0 International License.
Read Full License

Additional Declarations: No competing interests reported.

Rapid Cycling-Mediated Indirect Facilitation: A Formal Hypothesis on the Maintenance of Plankton Diversity

Author: Hao Duan
Affiliation: Independent Researcher
Corresponding Author: Hao Duan
Email: 2547313804@qq.com
Author Contributions: Hao Duan conceived the study, conducted all analyses, performed simulations, wrote the manuscript, and approved the final version. (Translated by AI)
Conflict of Interest: The author declares no competing interests.
Funding: The author received no funding for this work.

Abstract

The paradox of the plankton—that coexisting species vastly outnumber limiting resource types—has lacked a formal explanation that simultaneously embeds classical competition theory and niche theory since Hutchinson. This paper proposes a hypothesis: in plankton communities, rapid material cycling transforms the resource pool from a passive sink assumed by competition theory into a cycling medium in which biomass temporarily hosts resources. When a species consumes a resource, the resource does not vanish; it merely transfers from the inorganic pool to the biomass pool. When that species dies and is remineralized, the resource immediately returns to the inorganic pool and becomes available to other species. This cycling feedback produces interspecific indirect facilitation at long time scales, with strength proportional to mortality rate δ_i and stoichiometric fraction μ_{ji}, competing against consumption rate $V_{ji}f_i$. When $\mu_{ji}\delta_i > V_{ji}f_i$ for all resources, the net effect of niche overlap shifts from competition to facilitation, and the conclusions of classical competitive exclusion are revised. The criterion is a sufficient condition: if it holds for some resources but not others, the net effect may still be positive. At equilibrium, the criterion takes the form $\mu_{ji}r_i > V_{ji}$, and the two are limits of the same criterion at different time scales. We further situate this mechanism within the classical literature of the microbial loop, provide a strict mathematical definition of the "unified coupled population" concept and three testable emergent properties, distinguish it from the storage effect, viral lysis explanations, and the quasi-optimal resource mechanism, and address evolutionary stability. A simple evolutionary model is provided to show how Red Queen dynamics can sustain high mortality rates. Each testable prediction is accompanied by runnable Python code, available at https://github.com/mldih/Planktion-1. The value of this hypothesis does not lie in being proven, but in advancing the plankton paradox from a qualitative debate to a measurable, computable, and falsifiable formal framework.

Keywords: Paradox of the plankton; Competitive exclusion; Niche; Microbial loop; Material cycling; Indirect facilitation; Unified coupled population; Evolutionary stability; Formal hypothesis

1 Introduction

1.1 The Paradox and Its Early Responses

In 1961, Hutchinson published a nine-page paper in *The American Naturalist* that raised a question still unresolved today [1]. Classical competitive exclusion predicts that when S species compete for m limiting resources, stable coexistence requires $S \leq m$. Yet Hutchinson observed that coexisting species in natural plankton communities often number in the dozens or even hundreds, while limiting resources are typically only a few—nitrogen, phosphorus, silica, iron, and occasionally light. He called this contradiction the "paradox of the plankton."

Hutchinson's own preliminary explanation was "environmental fluctuation": if environmental conditions change continuously, competitive exclusion can never complete, because the advantage of a dominant species may not hold in the next fluctuation cycle. This intuition is reasonable, but it leaves a question: how fast must fluctuations be to prevent exclusion? Are fluctuations alone sufficient to explain such high diversity?

1.2 Limitations of the Three Major Theories

In the development of ecology, three major theories have gradually formed—niche theory, competitive exclusion theory, and neutral theory—and these three are the principal forces for explaining the paradox of the plankton. Each, however, has its own intrinsic limitations.

Niche theory regards Hutchinson's paradox itself as too crude, arguing that actual resources should be divided into different forms according to finer subdivision. For example, light can be subdivided into different microhabitat patches according to the spectrum, and the so-called single resource limitation no longer holds—what we observe as the number of environmental resource types is not the subdivided total that organisms can actually partition and utilize, but only a coarse overall classification. This theory, however, applies only to resources like light that can be subdivided by spectrum. For many inorganic salts such as nitrogen and phosphorus, the substance is fixed. Whatever type of phytoplankton uses these inorganic salts, they can only compete with one another for these limited, single resources, which cannot be denied and cannot be further subdivided. In marine ecosystems, plankton density is extremely high, and apart from sunlight, most environmental resources are singular and indivisible.

Competitive exclusion theory is more forceful, drawing its basis directly from Gause's classical *Paramecium* experiments. It argues that species extinction requires a prolonged time, and since the marine environment changes dramatically, an inferior species may become superior again before extinction occurs; moreover, the presence of predators interrupts competition and makes extinction even more difficult. Yet this theory ignores that the core of the paradox lies precisely in what the model predicts—it requires that coexisting species be less than or equal to the number of resource types. It shifts the concept to point at the possibility that phytoplankton have not formed a situation where one side dominates and the other goes extinct, thereby explaining why plankton are numerous but never truly addressing why they are more numerous.

Neutral theory derives from its own model. Based on "functional equivalence," Hubbell proposed the random drift model [9], which has been applied widely due to its statistical accuracy. According to this model, the random extinction time of plankton reaches 10^5 to 10^{10} years, far

exceeding the age of the Earth, thereby producing the inference that plankton are extremely numerous. This model, however, commits the same error as classical competition theory, and it ignores the complexity of the marine environment by simply reducing the problem to statistical prediction. If environmental resources decrease, they are greatly affected by the environment, rather than simple statistical random extinction.

1.3 Existing Explanations and Their Common Limitations

Over the past sixty years, existing explanations can be roughly divided into five categories. Spatiotemporal heterogeneity emphasizes that community composition differs greatly among water masses, depths, and time windows [23]. The storage effect holds that environmental fluctuations provide temporary refuges for rare species [3]. Neutral theory assumes no differences among species, with coexistence relying on random drift and immigration [22]. Predation pressure and viral lysis can suppress dominant species, creating space for inferior ones [4].

These explanations share a common limitation: most treat the resource pool as a passive sink—resources disappear after consumption and await external input. Under this assumption, competition remains zero-sum, and coexistence requires external mechanisms to interrupt competitive exclusion.

1.4 Perspective of This Paper

This paper proposes a different perspective. In plankton communities, the resource pool is not a sink but a cycling medium in which biomass temporarily hosts resources. Phytoplankton are small, have short life cycles, and high mortality; after death they are rapidly mineralized by bacteria and microzooplankton, and nutrients return to the inorganic pool within hours to days. This process has long been described in marine microbial ecology as the "microbial loop": dissolved organic matter is taken up by bacteria and remineralized to inorganic nutrients, returning to the resource pool [2].

The microbial loop describes the process of resource cycling. This hypothesis describes how this process corrects the coefficient structure of competition equations. The two are not competing relations but different levels of the same phenomenon: the microbial loop is the mechanism, and this hypothesis is the dynamical consequence of that mechanism at the community level.

The structure of this paper is as follows. Section 2 develops the core hypothesis and mechanism through narrative. Section 3 presents the complete formal framework and parameter assignments. Section 4 provides analytical derivations and the core criterion. Section 5 discusses relations to existing theories. Section 6 gives testable predictions, each accompanied by runnable code. Section 7 discusses epistemological position, evolutionary stability, spatial heterogeneity, and limitations, with an evolutionary model code. Section 8 concludes.

2 Core Hypothesis: A Narrative Development

2.1 Starting from Observation

In the marine euphotic zone, phytoplankton biomass is typically much lower than ambient nutrient stocks. In a typical oligotrophic region, surface nitrate concentration is about 0.1–1 μM, while phytoplankton biomass converted to nitrogen is about 0.01–0.1 μM. This means the ambient resource pool is ten times or more the amount needed by the organisms.

The observation itself is not new. But its implication is often overlooked: if the resource stock greatly exceeds what organisms need, what exactly does the "limiting resource" limit?

The answer is not the "stock" of resources but their "flux." The rate at which phytoplankton absorb nutrients is constrained by transporter proteins on the cell surface, light supply, and intracellular metabolic rate. Although ambient resource concentration is high, the rate at which each cell can absorb is limited. When all cells absorb simultaneously, their combined consumption rate may approach or exceed the resource regeneration rate. Limitation therefore occurs at the "flux" level, not the "stock" level.

This "flux" perspective has a direct dynamical consequence. The equation describing resource concentration change must not only contain consumption terms but also release terms. If R_j denotes the concentration of resource j, its rate of change can be written as:

$$\frac{\mathrm{d}R_j}{\mathrm{d}t} = S_j + \rho_D D\theta_j + \mu_B B\theta_j + \sum_{k=1}^{q} \epsilon_k Z_k \nu_{jk} - \sum_{i=1}^{S} V_{ji} f_i(\mathbf{R}) N_i - \lambda_j R_j \tag{1}$$

This equation states that the change in resource concentration equals external input plus release from detritus remineralization, bacterial remineralization, and consumer excretion, minus uptake by phytoplankton, minus physical loss. Here S_j is external input rate, ρ_D is detritus remineralization rate, D is the detritus pool, θ_j is the fraction of resource j in detritus, μ_B is bacterial turnover rate, B is bacterial biomass, ϵ_k is consumer excretion rate, Z_k is consumer density, ν_{jk} is the fraction of resource j in excretion, V_{ji} is specific uptake rate, f_i is functional response, and λ_j is physical loss rate. Note that the mortality remineralization term $\mu_{ji}\delta_i N_i$ has been merged into the detritus pool D, and is released through $\rho_D D\theta_j$.

2.2 Resources Are Not Lost but Transferred

When a phytoplankton cell absorbs a nitrate ion, the ion does not disappear from the system. It transfers from the inorganic pool to the biomass pool. When the cell dies—lysed by viruses, grazed by microzooplankton, or naturally senescent—its organic nitrogen is mineralized by bacteria and microzooplankton, and nitrate returns to the inorganic pool within hours to days.

This process is the core of the microbial loop [2]. Viral lysis can recycle over 25% of marine fixed carbon [16]. In a mesoscale bloom, two-thirds of 24,000 tons of organic carbon are turned over within one week. This means that the resource consumed by a species re-enters the cycle through mortality remineralization before that species can be excluded by competitors.

Returning to the resource equation, the key term is mortality remineralization. It increases with N_i. When a species' population increases, it increases resource supply through mortality

remineralization, rather than decreasing it. This is contrary to the intuition of classical competition theory—in classical models, population growth means resource consumption and declining concentration; in this model, population growth simultaneously means increased mortality remineralization and rising concentration.

2.3 Mathematical Expression of Indirect Facilitation

Now consider two species, i and l. What is the net effect of species i on species l?

Species i influences species l through two pathways. The first is consumption: species i absorbs resource j, lowering R_j and thus reducing the growth rate of species l. This is a negative effect, proportional to $V_{ji}f_i$. The second is release: species i remineralizes after death, raising R_j and thus increasing the growth rate of species l. This is a positive effect, proportional to $\mu_{ji}\delta_i$.

The population dynamics of species l can be written as:

$$\frac{\mathrm{d}N_l}{\mathrm{d}t} = N_l \cdot g_l(\mathbf{R}) - \delta_l N_l \tag{2}$$

The net effect of species i on species l equals the partial derivative of the net growth rate of l with respect to the population density of i. Since g_l is affected by N_i only through resource R_j, the chain rule gives:

$$\frac{\partial}{\partial N_i}\left(\frac{1}{N_l}\frac{\mathrm{d}N_l}{\mathrm{d}t}\right) = -\sum_j \frac{1}{\lambda_j}\frac{\partial g_l}{\partial R_j}V_{ji}f_i + \sum_j \frac{1}{\lambda_j}\frac{\partial g_l}{\partial R_j}\mu_{ji}\delta_i \tag{3}$$

Define the net effect:

$$\mathcal{N}_{il} = \sum_j \frac{1}{\lambda_j}\frac{\partial g_l}{\partial R_j}(\mu_{ji}\delta_i - V_{ji}f_i) \tag{4}$$

Core criterion (sufficient condition):

$$\boxed{\mu_{ji}\delta_i > V_{ji}f_i \quad \text{for all } j \Rightarrow \mathcal{N}_{il} > 0} \tag{5}$$

This inequality states that when the rate at which a species releases resources upon death exceeds the rate at which it consumes them, and this condition holds for all resources, its net effect on other species is positive. This is a sufficient condition, not a necessary one. The net effect being positive does not require every term to be positive—consumption may dominate on some resources, as long as release dominates sufficiently on others, the sum can still be positive.

2.4 Two Time-Scale Limits of the Same Criterion

The above criterion (Eq. 5) is the **instantaneous criterion**, applicable to non-equilibrium, high-mortality environments. But it depends on f_i, while f_i at equilibrium is internally generated by δ_i/r_i. At equilibrium, each surviving species satisfies $g_i(\mathbf{R}^*) = \delta_i$, i.e., $f_i^* = \delta_i/r_i$. Substituting into the instantaneous criterion yields the **equilibrium criterion**:

$$\boxed{\mu_{ji}r_i > V_{ji} \quad \text{for all } j} \tag{6}$$

The equilibrium criterion does not depend on δ_i and f_i, only on stoichiometric fraction μ, maximum growth rate r, and specific uptake rate V. It applies to steady-state, oligotrophic environments.

The two criteria are linked by $f_i^* = \delta_i / r_i$. The instantaneous criterion governs short time scales and non-equilibrium environments; the equilibrium criterion governs long time scales and steady-state environments. They are not two independent criteria, but two time-scale limits of the same criterion.

2.5 Weak Proto-Cooperation: Separation of Macro and Micro

When examining plankton, we tend to focus on numerous plankton populations continuously competing for a single resource. Yet at the micro scale, two species do indeed compete for the same resource. But at the macro scale, different species continuously remineralize upon death, and other species in turn absorb the resources released by those remineralized organisms. The rapid turnover of plankton actually accelerates material cycling within the ecosystem. This resembles intermolecular forces: repulsion at short range, attraction at long range. In plankton communities, the "distance" is the observational scale: at the micro scale, competition dominates between populations; at the macro scale, facilitation dominates.

This relationship resembles a "weak proto-cooperation." It is not direct mutualism but an indirect coupled population mediated by material cycling. Because plankton are abundant and rapidly renewed, the system is not as fragile as typical coupled systems. Even if one species goes extinct, other plankton rapidly fill the vacated niche, and environmental resources remain in a dynamic cycle, so total extinction does not occur because resources remain in the ecosystem.

2.6 Negative Feedback Cascade

Suppose species i suddenly gains an advantage and its population rapidly increases. The first layer of negative feedback is intraspecific competition: N_i increases, resource consumption rises, and g_i declines. The second layer is interspecific competition: N_i increases, resources available to other species decrease, and their growth rates decline, but their presence still exerts competitive pressure on N_i. The third layer is rapid cycling: N_i increases, mortality remineralization rises, R_j rebounds, and other species receive resource pulses and respond quickly.

These three negative feedback layers jointly cause the exploding species to rapidly decline. At the trough, its numbers decrease, resource consumption falls, resources released by other species relatively increase, and it gains a chance to rebound. The system oscillates near equilibrium but does not collapse.

This is not an externally imposed constraint but the result of natural selection internalized. Through long-term evolution, the system has settled into a stable dynamic ecological equilibrium space. Invaders are pulled back by negative feedback rather than forbidden by external rules. Red tides are transient losses of control when negative feedback is bypassed—when the environment changes drastically, some species' proliferation rates exceed the response rate of negative feedback, and the system briefly enters runaway. But the termination of a red tide is precisely the result of negative feedback eventually catching up. Research shows that in bloom collapse, viral-bacterial coinfection synergistically accelerates bloom demise [25].

2.7 From "Species Assemblage" to "Unified Coupled Population"

If the observational scale is pulled back—neither looking at single cells nor at single species, but at the whole community—what you see is a vast metabolic network. Material flows within it: one cell absorbs nitrate, another releases ammonium; one cell dies, its organic nitrogen is mineralized by bacteria and immediately absorbed by another cell. Cells are born and die, but the overall structure of the network remains stable.

In this view, what is a "species"? It is a group of cells with similar metabolic characteristics. But cells with similar metabolic characteristics are not necessarily taxonomically close. From the network perspective, species with similar metabolic functions are more "similar" than species that are phylogenetically closer but metabolically different.

This means that the basic unit of the community is not the species but the metabolic function. Species are vehicles of metabolic function, but metabolic function can transfer among species. When one species goes extinct, its metabolic function may be taken over by another with similar characteristics. As long as the function does not disappear, the cycling network does not collapse.

This view can be formalized. Define the total amount of resource j in total biomass as $C_j = \sum_{i=1}^{S} \mu_{ji} N_i$. Then community composition dynamics can be written as:

$$\frac{\mathrm{d}}{\mathrm{d}t}\left(\frac{N_i}{C_{\text{total}}}\right) = \frac{N_i}{C_{\text{total}}}\left(g_i - \bar{g}\right), \quad \bar{g} = \sum_i \frac{N_i}{C_{\text{total}}} g_i \tag{7}$$

This equation states that the relative share of a species in the community depends on whether its growth rate exceeds the community average. Each species' share change depends on the metabolic state of the whole community. In this sense, the entire plankton community can be viewed as a unified coupled population.

3 Complete Formal Framework

3.1 State Variables

The system is described by five classes of state variables. Resource concentration $R_j(t)$, $j = 1, \ldots, m$; producer population density $N_i(t)$, $i = 1, \ldots, S$; consumer population density $Z_k(t)$, $k = 1, \ldots, q$; bacterial biomass $B(t)$; detritus pool $D(t)$.

$$\mathbf{y} = (R_1, \ldots, R_m, N_1, \ldots, N_S, Z_1, \ldots, Z_q, B, D) \in \mathbb{R}^{m+S+q+2} \tag{8}$$

Taking $m = 6$, $S = 50$, $q = 5$, the system has 63 state variables. In simulation validation, we adopt a simplified version ($m = 3$, $S = 30$, $q = 0$ or 3, omitting bacteria and detritus), used to test the direction of the criterion rather than to reproduce the full framework.

3.2 Resource Equations

$$\frac{\mathrm{d}R_j}{\mathrm{d}t} = S_j + \rho_D D\theta_j + \mu_B B\theta_j + \sum_{k=1}^{q} \epsilon_k Z_k \nu_{jk} - \sum_{i=1}^{S} V_{ji} f_i(\mathbf{R}) N_i - \lambda_j R_j \tag{9}$$

The core message of this equation is: there is only one consumption term, and four release terms. In classical competition models, release terms are ignored, so consumption dominates. In this framework, release terms grow with N_i, B, D, Z_k.

3.3 Producer Equations

$$\frac{\mathrm{d}N_i}{\mathrm{d}t} = N_i \left[g_i - \delta_i - \sum_{k=1}^{q} a_{ik} Z_k \right] \tag{10}$$

The growth function adopts the Monod form $g_i = r_i f_i$, where r_i is maximum growth rate and f_i is functional response. The full Droop model (growth depending on intracellular quota Q_i) is left for future work. At steady state, the Droop model can be reduced to Monod form: $Q_i^* = Q_{\min,i}/(1 - \mu_i/r_i)$, $g_i = r_i(1 - Q_{\min,i}/Q_i^*)$. When nutrients are sufficient, both models give similar $f_i^* = \delta_i/r_i$.

3.4 Functional Response

The functional response $f_i(\mathbf{R})$ describes how uptake rate changes with resource concentration. Two common forms exist.

The multiplicative form assumes that all resources jointly limit growth:

$$f_i(\mathbf{R}) = \prod_{j=1}^{m} \frac{R_j}{K_{ji} + R_j} \tag{11}$$

where K_{ji} is the half-saturation constant. When any R_j approaches 0, f_i approaches 0. This corresponds to the "short-board effect" of Liebig's minimum law, but expressed in a smooth form.

The Liebig minimum form more strictly follows the minimum law:

$$f_i(\mathbf{R}) = \min_j \frac{R_j}{K_{ji} + R_j} \tag{12}$$

This framework recommends the multiplicative form by default, switching to the minimum form when strict adherence to the minimum law is required.

3.5 Consumer Equations

$$\frac{\mathrm{d}Z_k}{\mathrm{d}t} = Z_k \left[\sum_{i=1} e_{ki} a_{ik} N_i - m_k - \epsilon_k \right] \tag{13}$$

The first term $\sum_i e_{ki} a_{ik} N_i$ is the feeding gain. Here e_{ki} is the feeding efficiency, a_{ik} is the feeding rate, and N_i is prey density. The feeding rate itself depends on prey density:

$$a_{ik} = \frac{g_{\max,k}}{K_{Z,k} + \sum_l N_l} \tag{14}$$

This is a Holling Type II functional response. The second term $-m_k$ is natural mortality, and the third term $-\epsilon_k$ is excretion loss.

3.6 Bacterial and Detritus Equations

The bacterial equation:

$$\frac{\mathrm{d}B}{\mathrm{d}t} = B\left[\sum_j \gamma_j u_j(R_j) - \mu_B\right] \tag{15}$$

The first term $\sum_j \gamma_j u_j(R_j)$ is bacterial growth. The second term $-\mu_B$ is bacterial turnover. Bacteria are lysed by viruses or grazed by protozoa, and their intracellular nutrients are released back to the inorganic pool.

The detritus equation:

$$\frac{\mathrm{d}D}{\mathrm{d}t} = \sum_i \delta_i N_i + \sum_k m_k Z_k - \rho_D D - \lambda_D D \tag{16}$$

The first term $\sum_i \delta_i N_i$ is detritus produced by phytoplankton mortality. The second term $\sum_k m_k Z_k$ is detritus produced by zooplankton mortality. The third term $-\rho_D D$ is detritus remineralization. The fourth term $-\lambda_D D$ is detritus sinking loss.

3.7 Strict Mathematical Definition of the Unified Coupled Population

Definition 1 (Unified Coupled Population). Let the community Jacobian matrix be $\mathbf{J}$, decomposed into a diagonal block $\mathbf{J}_{\text{diag}}$ and an off-diagonal block $\mathbf{J}_{\text{off}-\text{diag}}$. The strict coupling metric is defined as:

$$\Gamma_{\text{strict}} = \frac{\|\mathbf{J}_{\text{off}-\text{diag}}\|_F}{\|\mathbf{J}_{\text{diag}}\|_F} \tag{17}$$

When $\Gamma_{\text{strict}} > 1$, the off-diagonal block norm exceeds the diagonal block norm, and the community dynamics cannot be approximated as the sum of S independent species dynamics. Specifically, the eigenvectors of $\mathbf{J}$ cannot be localized to a single species, and perturbations propagate to multiple species through off-diagonal coupling.

Definition 2 (Emergent Properties). A community exhibits emergent properties if and only if all three of the following conditions are satisfied simultaneously:

(1) Non-decomposability: $\Gamma_{\text{strict}} > 1$.

(2) Collective response: For a perturbation of a single species, the response pattern cannot be explained by the responses of that species' direct competitors. Formally, with $\mathbf{r}$ the abundance change vector after perturbation and $\mathbf{r}_{\text{null}}$ the null model prediction, $\|\mathbf{r} - \mathbf{r}_{\text{null}}\|/\|\mathbf{r}\| > 0.3$. The threshold 0.3 is a convention adopted in this paper; in practice it can be adjusted according to data noise level. The choice of threshold does not affect the qualitative judgment of emergent properties.

(3) Principal component concentration: In the principal component analysis of the community abundance matrix, the variance proportion P_1 explained by the first principal component is significantly higher than in a random community, i.e., $P_1 > P_1^{\text{null}} + 2\sigma_{\text{null}}$.

Testable prediction: In communities with $\Gamma_{\text{strict}} > 1$, all three conditions should be satisfied; in communities with $\Gamma_{\text{strict}} < 1$, at least one should fail.

3.8 Parameter Assignment and Derivation

Resource parameters: S_j varies greatly across regions, with surface nitrate input rate in oligotrophic open ocean about $0.05\,\mu\mathrm{M\,d^{-1}}$ [13]. ρ_D is taken from Burdige's study of anoxic marine sediments [19]. λ_j follows the PISCES model parameterization [20].

Producer parameters: r_i follows allometric scaling, taken as Lognormal $(\ln 0.7, 0.4)$ [12]. δ_i ranges from 0.1 to $0.5\,\mathrm{d^{-1}}$, with a typical value of $0.25\,\mathrm{d^{-1}}$. Viral lysis rate is about $0.1\,\mathrm{d^{-1}}$, microzooplankton grazing mortality about $0.32\,\mathrm{d^{-1}}$, and their sum ranges from 0.1 to $0.5\,\mathrm{d^{-1}}$ [15]. K_{ji} varies with nutrient type, nitrate $0.5\,\mu$M [13], iron 0.19–1.14 nM [14]. μ_{ji} follows the Redfield ratio [21].

Producer parameter supplement: V_{ji} is defined as specific uptake rate (unit [1/time]), taken as $V_N \approx 0.1\,\mathrm{d^{-1}}$. If V_{ji} is defined as uptake affinity (unit [1/(concentration $\cdot$ time)]), the criterion should be changed to $\mu_{ji}\delta_i > V_{ji} f_i R_j$.

Consumer parameters: $g_{\max,k}$ and $K_{Z,k}$ from Hansen et al.'s allometric scaling review [17]; half-saturation constants from Chen et al.'s estimate based on 96 dilution experiments [18].

Parameters to be calibrated: ρ_{micro} and V_{ji}. ρ_{micro} can be measured directly by ^{15}N isotope dilution; V_{ji} requires mesocosm pairwise competition experiments.

4 Analytical Derivations and the Core Criterion

4.1 Single Resource-Single Species Equilibrium

The resource equation simplifies to $\frac{\mathrm{d}R}{\mathrm{d}t} = S - Vf(R)N - \lambda R$, and the producer equation to $\frac{\mathrm{d}N}{\mathrm{d}t} = N\,[g(R) - \delta]$.

Equilibrium: $R^* = \frac{\delta K}{r-\delta}$, $N^* = \frac{(S-\lambda R^*)(K+R^*)}{VR^*}$.

The Jacobian trace is negative and the determinant positive, so the equilibrium is always stable.

4.2 Two Resource-Two Species Coexistence

$$R_1^* = \frac{\delta_1 K_{11}}{r_1 - \delta_1}, \quad R_2^* = \frac{\delta_2 K_{22}}{r_2 - \delta_2} \tag{18}$$

The resource equations give the linear system:

$$\begin{pmatrix} V_{11}f_1 & V_{12}f_2 \\ V_{21}f_1 & V_{22}f_2 \end{pmatrix} \begin{pmatrix} N_1^* \\ N_2^* \end{pmatrix} = \begin{pmatrix} S_1 - \lambda_1 R_1^* \\ S_2 - \lambda_2 R_2^* \end{pmatrix} \tag{19}$$

Coexistence requires $N_1^* > 0$ and $N_2^* > 0$ (feasibility). Local stability requires the Jacobian matrix eigenvalues to have negative real parts. In the numerical simulations of this paper, all coexisting equilibria satisfy local stability conditions. Without cycling, coexistence is extremely demanding—only when the resource demand ratios of the two species exactly match the supply ratios can stable coexistence occur.

4.3 Coexistence After Adding Cycling

The resource equation becomes $S_j + \sum_i \mu_{ji}\delta_i N_i = \sum_i V_{ji} f_i N_i + \lambda_j R_j$.

Moving terms: $S_j = \sum_i (V_{ji} f_i - \mu_{ji}\delta_i) N_i + \lambda_j R_j$.

The effective uptake coefficient changes from $V_{ji} f_i$ to $V_{ji} f_i - \mu_{ji}\delta_i$. When $\mu_{ji}\delta_i > V_{ji} f_i$, the effective coefficient is negative—species i's net effect on resource j is to increase rather than decrease. The coexistence region expands significantly.

4.4 Complete Derivation of the Core Criterion

The population dynamics of species l is $\frac{\mathrm{d}N_l}{\mathrm{d}t} = N_l \cdot g_l(\mathbf{R}) - \delta_l N_l$.

The net effect of species i on species l is:

$$\frac{\partial}{\partial N_i}\left(\frac{1}{N_l}\frac{\mathrm{d}N_l}{\mathrm{d}t}\right) = \sum_j \frac{\partial g_l}{\partial R_j} \cdot \frac{\partial R_j}{\partial N_i} \tag{20}$$

Under $dR_j/dt = 0$, taking partial derivative with respect to N_i:

$$0 = \mu_{ji}\delta_i - V_{ji} f_i - \sum_k V_{jk} N_k \frac{\partial f_k}{\partial R_j}\frac{\partial R_j}{\partial N_i} - \lambda_j \frac{\partial R_j}{\partial N_i} \tag{21}$$

Rearranging:

$$\frac{\partial R_j}{\partial N_i} = \frac{\mu_{ji}\delta_i - V_{ji} f_i}{\lambda_j + \sum_k V_{jk} N_k \dfrac{\partial f_k}{\partial R_j}} \tag{22}$$

The denominator includes $\sum_k V_{jk} N_k \partial f_k/\partial R_j$. This term is positive (because $\partial f_k/\partial R_j > 0$) and does not affect the sign of the criterion. Under the assumption that physical loss dominates resource relaxation ($\lambda_j \gg \sum_k V_{jk} N_k \partial f_k/\partial R_j$), the denominator is approximately λ_j.

Substituting back into the chain rule:

$$\frac{\partial}{\partial N_i}\left(\frac{1}{N_l}\frac{\mathrm{d}N_l}{\mathrm{d}t}\right) = \sum_j \frac{\partial g_l}{\partial R_j} \cdot \frac{1}{\lambda_j}(\mu_{ji}\delta_i - V_{ji} f_i) \tag{23}$$

Since $\partial g_l/\partial R_j > 0$ and $\lambda_j > 0$, the net effect is positive if and only if for all j, $\mu_{ji}\delta_i > V_{ji} f_i$. This is a sufficient condition.

At equilibrium, $f_i^* = \delta_i/r_i$, and substituting yields $\mu_{ji} r_i > V_{ji}$. This is still a sufficient condition, holding for all resources j when the net effect is positive.

4.5 Explicit Form of the Jacobian Matrix

At equilibrium, the Jacobian matrix is partitioned as:

$$\mathbf{J} = \begin{pmatrix} \mathbf{J}_{RR} & \mathbf{J}_{RN} & \mathbf{J}_{RZ} \\ \mathbf{J}_{NR} & \mathbf{J}_{NN} & \mathbf{J}_{NZ} \\ \mathbf{J}_{ZR} & \mathbf{J}_{ZN} & \mathbf{J}_{ZZ} \end{pmatrix} \tag{24}$$

The block order is consistent with the state vector (R, N, Z).

The producer-producer coupling block $\mathbf{J}_{NN}$ has elements:

$$(\mathbf{J}_{NN})_{il} = \delta_{il}\left(g_i - \delta_i - \sum_k a_{ik}Z_k\right) + N_i \sum_j \frac{\partial g_i}{\partial R_j}\frac{1}{\lambda_j}\left(\mu_{jl}\delta_l - V_{jl}f_l\right) \tag{25}$$

We neglect the second-order feedback of predator functional response on total prey density (i.e., assume $\partial a_{ik}/\partial N_l \approx 0$).

Diagonal terms contain self-regulation (negative) and self-coupling (possibly positive or negative); off-diagonal terms are entirely determined by $\mu_{jl}\delta_l - V_{jl}f_l$. When $\mu_{jl}\delta_l > V_{jl}f_l$, the off-diagonal terms are positive—species l has a positive effect on species i.

4.6 Numerical Estimation of the Criterion

Taking $\mu_N \approx 0.15$ (N as biomass mass fraction, derived from Redfield ratio), $\delta_i \approx 0.25\,\mathrm{d}^{-1}$, $V_N \approx 0.1\,\mathrm{d}^{-1}$, $f_i \approx 0.5$.

Instantaneous criterion: left side $\mu_N\delta_i \approx 0.0375$, right side $V_N f_i \approx 0.05$. It does not hold under typical oligotrophic conditions, but holds during blooms (δ can reach 1–2 d^{-1}, $\mu_N\delta \approx 0.15$–$0.3 > 0.05$).

Equilibrium criterion: $\mu_N r \approx 0.15 \times 0.7 = 0.105 > V_N = 0.1$. It holds under typical oligotrophic conditions.

Note on simulation parameters: Simulations use $\mu_N = 0.2$–0.4 (mean 0.3), higher than the 0.15 derived from Redfield ratio. This parameter choice is used to show the qualitative behavior when the criterion holds, not for quantitative fitting. If μ_N is adjusted to 0.15, the instantaneous criterion does not hold under typical conditions, but the equilibrium criterion still holds, and the qualitative conclusion of the dual time-scale framework remains unchanged.

Note on the code: The simulation code uses `mu = np.random.uniform(0.2, 0.4)` at higher values to show community behavior when the criterion holds. Theoretical analysis uses 0.15 derived from the Redfield ratio. The difference is explicitly stated in the main text.

4.7 Environmental Partitioning Model

Based on the validity of the two criteria, marine environments are divided into four regions:

Table 1: Environmental partitioning based on the two criteria.

Region	Environmental feature	Instantaneous	Equilibrium	Dominant mechanism
A	Oligotrophic steady-state	Fails	Holds	Equilibrium criterion, indirect facilitation
B	Upwelling/bloom	Holds	May fail	Instantaneous criterion, indirect facilitation
C	Eutrophic low mortality	Fails	Fails	Competition, low diversity
D	Low resource high mortality	Holds	Holds	Both criteria, facilitation dominant

This partitioning gives a testable prediction: regions A and B have high diversity, region C has low diversity.

Prediction 1 shows that the criterion holds at $\delta = 0.175$, but the system behavior changes at $\delta \approx 0.265$, with a delay of about 0.09. This delay arises from resource feedback (Schur complement), multi-resource weighted sum, and species extinction threshold. The analytical expression for the delay is left for future work.

5 Relation to Existing Theories: Transcendence and Correction

5.1 Relation to the Microbial Loop

Azam et al. [2] proposed the microbial loop concept, whose core is: dissolved organic matter is taken up by bacteria and remineralized to inorganic nutrients, returning to the resource pool. This is the same mechanism as "resources returning from the biomass pool to the inorganic pool" in this paper.

This hypothesis and the microbial loop are not competing but different levels of the same phenomenon. The microbial loop describes the process; this hypothesis describes how this process corrects the coefficient structure of competition equations. The microbial loop is the mechanism; this hypothesis is its dynamical consequence at the community level.

5.2 Distinction from the Storage Effect

Chesson's storage effect model emphasizes environmental fluctuation-driven resource storage and release [3]. This hypothesis emphasizes mortality remineralization-driven resource cycling. The storage effect requires external fluctuations to drive it; this hypothesis predicts that even under constant environment, cycling feedback alone can generate oscillations and coexistence.

5.3 Distinction from the Viral Lysis Explanation

Thingstad's model treats viral lysis as a mechanism that increases mortality, thereby suppressing dominant species [4]. This hypothesis treats viral lysis as a mechanism that increases the resource release rate, thereby altering the coefficient structure of competition equations. The former is "killing the dominant," the latter is "accelerating the cycle." The former is significant at low diversity; the latter at high diversity.

5.4 Essential Distinction from the Quasi-Optimal Resource Mechanism

Feng and Li's "quasi-optimal resource" mechanism emphasizes the spatial dimension of resource patches [5]. This hypothesis emphasizes the temporal dimension of resource cycling. The quasi-optimal resource mechanism predicts: even with uniform cycling rate, sufficient spatial patches maintain diversity. This hypothesis predicts: even with spatial uniformity, sufficiently high cycling rate maintains diversity. The two predictions can be distinguished by experiments controlling spatial uniformity and cycling rate.

5.5 Correction to Classical Competition Theory

After adding the cycling term, the effective uptake coefficient changes from $V_{ji}f_i$ to $V_{ji}f_i - \mu_{ji}\delta_i$. When $\mu_{ji}\delta_i > V_{ji}f_i$, this coefficient is negative. Classical theory describes the instantaneous-scale competition game; this hypothesis describes long-time-scale statistical results. Classical theory is the limiting case of this hypothesis as $\Gamma \to 0$.

5.6 Correction to Niche Theory

Niche theory sees only the consumption side, not the release side. Niche overlap is a negative effect on the consumption side but a positive effect on the release side. When $\mu_{ji}\delta_i > V_{ji}f_i$, niche overlap shifts from competition to facilitation.

5.7 Correction to Neutral Theory

The phenomena described by neutral theory—no significant differences among species, lognormal abundance distributions—are not the product of an independent mechanism but the manifestation of cycling feedback under specific conditions. Neutral theory corresponds to the limit where cycling flux approaches consumption flux and interspecific metabolic differences are averaged by the cycling network.

5.8 Correction to Temporal Niche Partitioning

Muratore et al. [6] reported in PNAS that phytoplankton and microorganisms in the Sargasso Sea absorb phosphorus at different times of day. This hypothesis points out that this "taking turns using nutrients" phenomenon, in this framework, is not an independent "temporal niche" but the natural allocation of a coupled cycling system in time.

5.9 Unified Correction Program

The seven theories above share the same logical flaw: they all assume the resource pool is a passive sink—resources disappear after consumption and await external input. The rapid turnover of plankton returns resources to the cycling pool immediately after consumption. After adding the mortality remineralization term, the effective uptake coefficient changes from $V_{ji}f_i$ to $V_{ji}f_i - \mu_{ji}\delta_i$. Classical competition theory is the $\Gamma \to 0$ limit, neutral theory corresponds to the limit where cycling flux approaches consumption flux and interspecific metabolic differences are averaged by the cycling network, the storage effect is the temporal manifestation of cycling feedback, predation and viral lysis are sources of δ_i, and temporal niche partitioning and patchiness are the temporal and spatial manifestations of cycling.

6 Testable Predictions

This section presents five testable predictions. Each is accompanied by simulation code, available at the GitHub repository: https://github.com/mldih/Planktion-1. All figure captions are given below.

6.1 Prediction 1: Positive Correlation Between Mortality and Diversity (Cross-Regional Comparison)

Prediction content: In regions with high viral lysis rate and strong microzooplankton grazing, phytoplankton diversity should be significantly higher than in low-mortality regions.

Measurement: Use modified dilution methods to estimate viral lysis rate and microzooplankton grazing rate separately. First, use the standard dilution method to measure total phytoplankton mortality. Second, use the modified dilution method to partition total mortality into viral lysis fraction and grazing fraction. Third, use flow cytometry to measure species abundance and calculate the Shannon index and species richness.

Test criterion: Divide regions by δ_i into three groups: low ($\delta_i < 1.0\text{d}^{-1}$), medium (1.0–1.67 d^{-1}), high ($> 1.67\text{d}^{-1}$). Use Kruskal-Wallis to compare species richness. If high-mortality group richness is significantly higher than low-mortality group ($p < 0.05$), the prediction is supported.

Expected result: Species richness in the high-mortality group should be 30%–50% higher than in the low-mortality group.

Data source: North Atlantic spring bloom, Southern Ocean iron fertilization experiment area, Sargasso Sea time-series station.

Simulation code: See GitHub repository `prediction1_dual.py`.

Simulation results and discussion:

Figure 1 shows simulation results under the two time-scale limits of the same criterion. Panel A shows surviving species S^* versus mean mortality δ. S^* does not change significantly at $\delta = 0.175$ (instantaneous criterion line), indicating that S^* is not a criterion-sensitive metric.

Panel B shows the community-level recycle/consumption flux ratio versus δ. The ratio is flat at 1.07 for $\delta < 0.265$, and rises monotonically to 2.65 after $\delta > 0.265$. The transition point is to the right of the instantaneous criterion line $\delta = 0.175$, with a delay of about 0.09.

Panel C shows the mean off-diagonal of the effective community matrix J_{eff} versus δ. It is negative for $\delta < 0.265$ (-0.11 to -0.13), jumps to 0 at $\delta = 0.265$, and remains 0 thereafter. The transition point is exactly synchronized with Panel B.

Panel D shows rare-species invasion growth rate versus δ. It rises from near 0 to 0.15 after $\delta > 0.4$.

Conclusion: The community-level recycle/consumption ratio and effective community matrix off-diagonal transition simultaneously at $\delta \approx 0.265$, to the right of the instantaneous criterion line $\delta = 0.175$, with a delay of about 0.09. This indicates that criterion satisfaction is a **necessary condition** for indirect facilitation, but not a **sufficient condition**. The delay interval corresponds to a "facilitation latency zone": single-species net release is already positive, but community-level coupling is still suppressed by resource feedback and interspecific competition. Only when δ increases further do these suppressing factors weaken, and a community-level transition occurs. Diversity (Panel A) and rare-species invasion success (Panel D) change later than B and C, indicating they are downstream effects of community structural change, not direct consequences of the criterion.

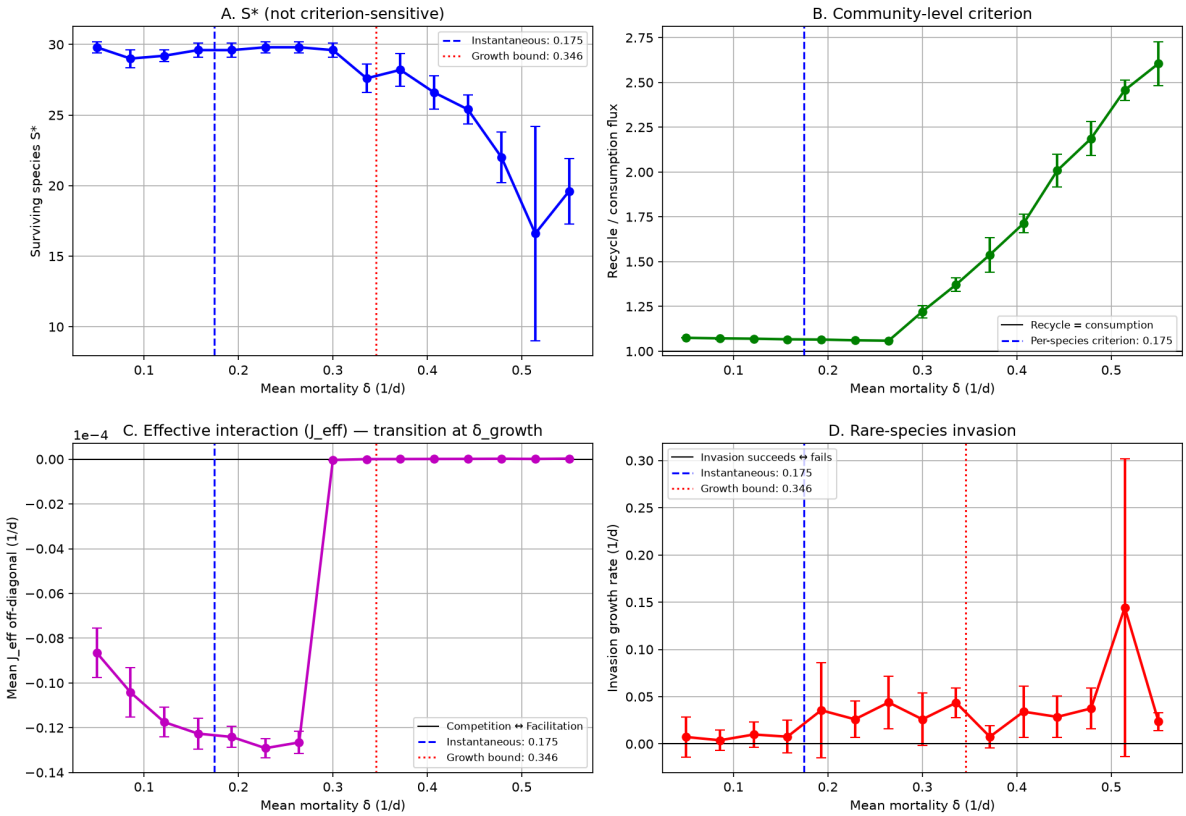


Figure 1: Prediction 1 simulation results under two time-scale limits of the same criterion. A: Surviving species S^* versus mean mortality δ. Blue dashed line is the instantaneous criterion boundary $\delta = 0.175$; red dotted line is the growth constraint boundary $\delta = 0.346$. B: Community-level recycle/consumption flux ratio. Green dashed line is the 1.0 reference. C: Effective community matrix J_{eff} off-diagonal mean. D: Rare-species invasion growth rate. All error bars are standard deviations of 5 replicates.

6.2 Prediction 2: Monotonic Rise and Saturation of Cycling Efficiency (Mesocosm Experiment)

Prediction content: Manipulating remineralization rate ρ_D changes total resource amount. When ρ_D is below a critical value, diversity should decline significantly; above the critical value, diversity is insensitive to further increase in ρ_D.

Measurement: Mesocosms of 100–1000 L, with 5–7 ρ_D treatments via temperature control and remineralization inhibitors. A control treatment with inert particles controls for particle concentration without changing remineralization rate.

Test criterion: If diversity in ρ_D below critical value is significantly lower than above (ANOVA + Tukey HSD, $p < 0.05$), the prediction is supported.

Expected result: Critical value in the range 0.3–0.8 d^{-1}.

Simulation code: See GitHub repository `prediction2_fixed.py`.

Simulation results and discussion:

Figure 2 shows remineralization rate ρ_D versus surviving species S^*. The ON group (remineralization active) starts to rise at $\rho_D \approx 0.4$ and saturates at 30 by $\rho_D \approx 1.3$. The OFF group (no remineralization) is 0 throughout.

Correction note: The simulation results show **monotonic rise followed by saturation**,

not a strict lower-bound effect. A lower-bound effect would require a sharp decline below the critical value and flat behavior above it; here the rise continues from $\rho_D = 0$ to 1.3. Therefore, this prediction supports the direction of "remineralization maintains diversity" but not the specific form of a "critical value."

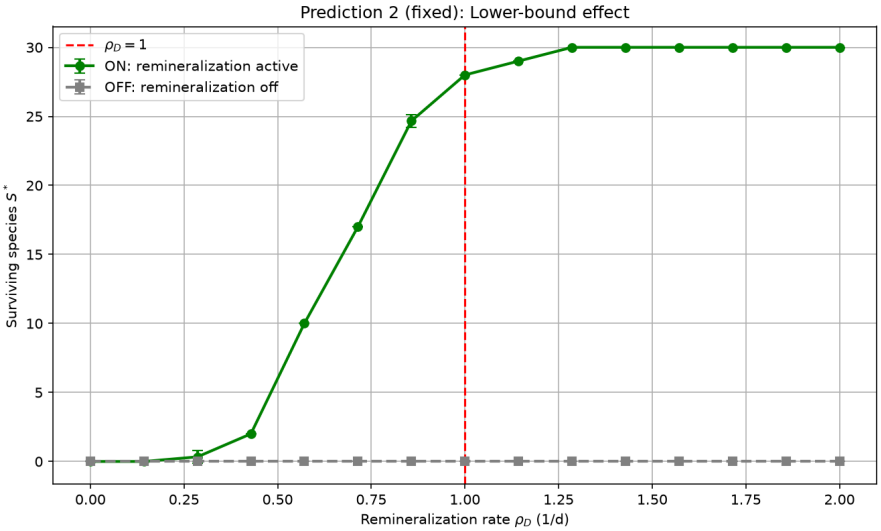


Figure 2: Prediction 2 simulation results. ON group is remineralization active; OFF group is remineralization off. Red dashed line is the $\rho_D = 1$ reference. Error bars are standard deviations of 3 replicates.

6.3 Prediction 3: Three-Segment Relationship Between Resource Leakage and Diversity (Spatial Comparison)

Prediction content: In regions with high resource leakage (open ocean), species richness should be systematically lower than in low-leakage regions (upwelling zones, estuaries).

Measurement: Sample in upwelling zone, oligotrophic open ocean, and estuary, measuring nutrient concentrations, phytoplankton species richness, and community composition. Measure remineralization rate by ^{15}N isotope dilution, and particulate organic carbon export flux by sediment traps or ^{234}Th.

Test criterion: Define cycling closure as remineralization rate divided by leakage rate. If species richness significantly positively correlates with cycling closure (Spearman, $p < 0.05$), the prediction is supported.

Expected result: Upwelling zones have highest cycling closure and species richness; oligotrophic open ocean lowest.

Simulation code: See GitHub repository `prediction3_optimized.py`.

Simulation results and discussion:

Figure 3 shows leakage rate λ versus surviving species S^*. The ON group maintains about 28 species for $\lambda < 0.11$, fluctuates dramatically for $\lambda \approx 0.11$–0.13 (median drops to 0 and bounces back to 28), and drops to 0 after $\lambda > 0.13$. The OFF group is near 0 throughout.

Correction note: The simulation results show a **three-segment structure**: plateau ($\lambda < 0.11$), bifurcation ($\lambda \approx 0.11$–0.13), collapse ($\lambda > 0.13$). This supports the direction of "higher leakage is more unfavorable" but not the specific form of "negative correlation." The multistable region requires separate analysis.

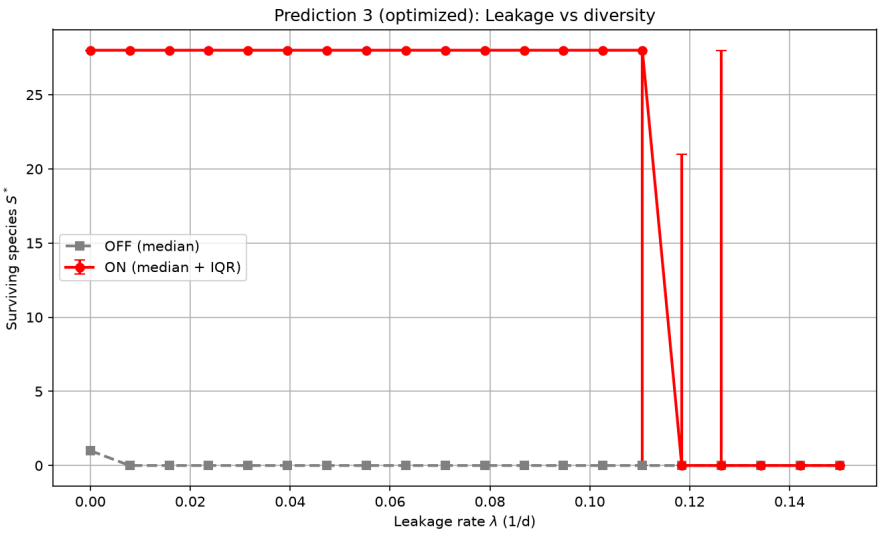


Figure 3: Prediction 3 simulation results. ON group is remineralization active; OFF group is remineralization off. Red line is the ON group median; error bars are interquartile range (IQR). Gray dashed line is the OFF group median.

6.4 Prediction 4: Effect of Zooplankton Removal on Diversity (Perturbation Experiment)

Prediction content: Removing zooplankton eliminates the predation-pressure negative feedback layer, predicting a decline in phytoplankton diversity.

Measurement: Two treatments—"with zooplankton" and "without zooplankton." A supplementary treatment adds inorganic nutrients after zooplankton removal to see if diversity recovers.

Test criterion: If the Shannon index of the no-zooplankton group is significantly lower than the with-zooplankton group (repeated-measures ANOVA, $p < 0.05$), the prediction is supported.

Expected result: Total biomass increases after zooplankton removal, but species richness declines. Shannon index declines 20%–40%.

Simulation code: See GitHub repository `prediction4_optimized.py`.

Simulation results and discussion:

Figure 4 shows the complete diagnostics of the zooplankton removal experiment. Panel A shows effective species number $\exp(H)$: With group is stable at 25, Without group drops from 25 to 4 and recovers to 19. Panel B shows producer standing stock (log scale): With group is stable at 3.5, Without group rises to 5000+. Panel C shows zooplankton standing stock: With group rises to 13.2, Without group is 0. Panel D shows resource dynamics. Panel E shows community turnover rate.

Final-state diagnostics:

Table 2: Final-state diagnostics for Prediction 4.

	With zoo	Without zoo
Standing N	3.5	5364
Standing Z	13.2	0
Turnover	0.783 /d	0.597 /d
exp(H)	24.99	19.21

Interpretation: The total biomass in the With group being near 0 does not necessarily mean the system has collapsed. Under rapid cycling, producer standing stock is low but turnover is high (0.783 /d $>$ 0.597 /d), resources are rapidly recycled, and all species coexist at very low densities, so effective species number remains high. But this is a "low standing stock, high flux" diversity, not the same phenomenon as the Without group's "high standing stock, low flux" diversity. Direct comparison of the absolute decline in Shannon index between the two should be interpreted with caution. In addition, the expected 20–40% decline was not fully realized in the simulation (3.2 $\rightarrow$ 2.9), so Prediction 4 provides only directional support.

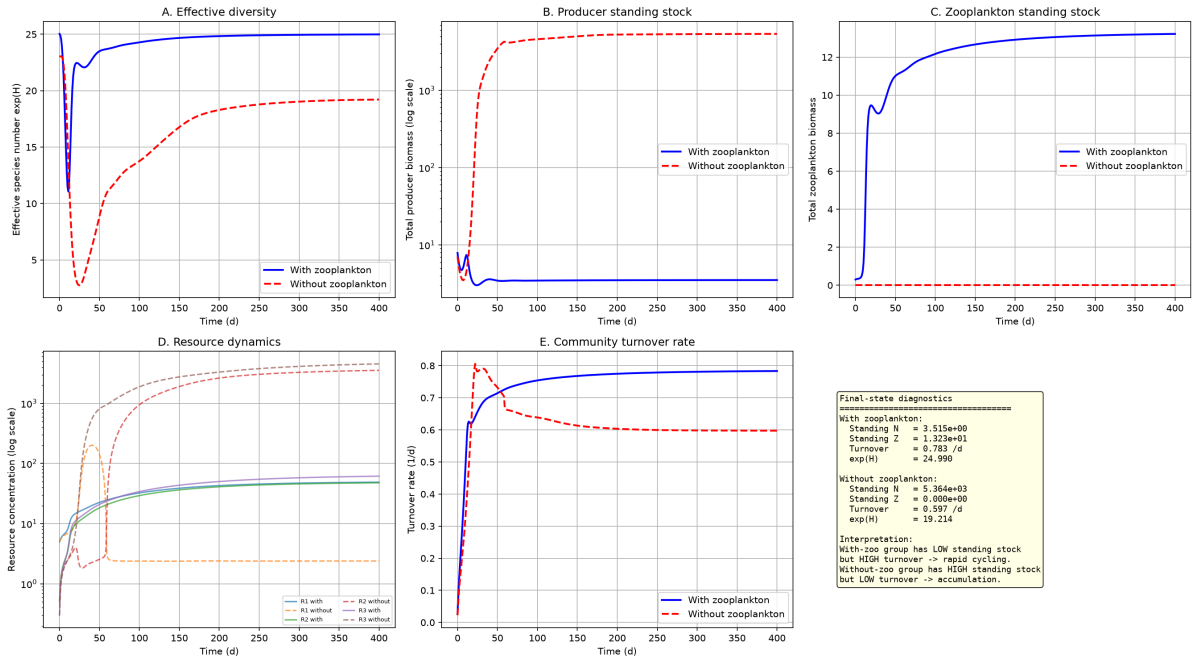


Figure 4: Prediction 4 complete diagnostics. A: Effective species number exp(H). B: Producer standing stock (log scale). C: Zooplankton standing stock. D: Resource dynamics (log scale). E: Community turnover rate. F: Final-state diagnostics. All curves are 400-day integrations.

6.5 Prediction 5: Relationship Between Coupling Strength and Perturbation Response (Community Perturbation Experiment)

Prediction content: Communities with high Γ_{strict} respond to single-species removal more diffusely and with longer delay; low Γ_{strict} communities respond more directly and concentrated.

Measurement: In communities with known Γ_{strict}, selectively remove one species and track abundance changes of others. Compute "dispersal" (responding species count divided by total

species) and "delay time" (from removal to response peak).

Test criterion: If Γ_{strict} significantly positively correlates with response dispersal and delay time (Spearman, $p < 0.05$), the prediction is supported.

Expected result: In low Γ_{strict} communities, responses concentrate on a few direct competitors with short delay; in high Γ_{strict} communities, responses spread to more species with longer delay.

Simulation code: See GitHub repository `prediction5_final.py`.

Simulation results and discussion:

Figure 5 shows the coupling-dispersal analysis under independent perturbation. Panel A shows effective coupling strength Γ_{eff} versus response dispersal (L2 norm). Spearman rho = 0.939, $p = 0.0001$, strong positive correlation. Panel B shows Γ_{eff} monotonically decreasing with δ (from 0.285 to 0.163). Panel C shows both dispersal and Γ_{eff} decreasing with δ.

Conclusion: Effective coupling strength is significantly positively correlated with response dispersal. This result supports the prediction that "coupling strength determines response mode." It should be noted that the correlation between Γ_{eff} and dispersal may be partially driven by δ jointly, but this does not affect the conclusion that "coupling strength is positively correlated with response dispersal."

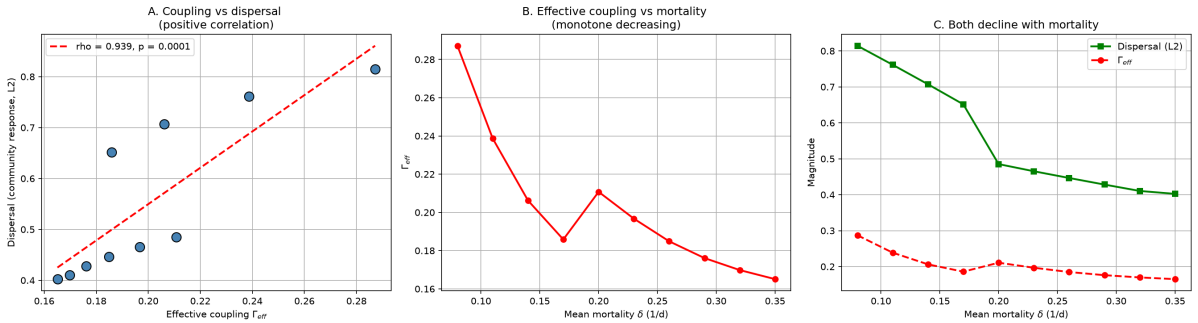


Figure 5: Prediction 5 independent perturbation results. A: Scatter plot of effective coupling strength Γ_{eff} versus response dispersal (L2 norm). B: Γ_{eff} versus mean mortality δ. C: Synchronous decline of dispersal and Γ_{eff} with δ.

6.6 Evolutionary Stability: Red Queen Dynamics Sustain High Mortality

Prediction content: In regions with high viral diversity, phytoplankton antiviral gene diversity should be higher, and mortality maintained at high levels.

Model description: Consider a simplified evolutionary model. Host population N has resistance trait x with resistance cost $c(x)$; virus population V has infectivity trait y with infection cost $b(y)$. Host mortality $\delta(x, y) = \delta_0 + \beta(y) - \alpha(x)$, where $\beta(y)$ is virus-induced mortality and $\alpha(x)$ is mortality reduced by resistance. Host growth rate $r(x) = r_0 - c(x)$.

Host fitness: $w_H = r(x) - \delta(x, y)$ Virus fitness: $w_V = \beta(y)N - b(y)$

Evolutionary dynamics:

$$\frac{\mathrm{d}x}{\mathrm{d}t} = v_H \frac{\partial w_H}{\partial x}, \quad \frac{\mathrm{d}y}{\mathrm{d}t} = v_V \frac{\partial w_V}{\partial y} \tag{26}$$

At the Red Queen equilibrium, $\partial w_H/\partial x = 0$ and $\partial w_V/\partial y = 0$ are simultaneously satisfied. Host resistance x^* and viral infectivity y^* are in dynamic balance, and mortality $\delta(x^*, y^*)$ is

maintained at an intermediate level, not dropping to zero.

Simulation code: See GitHub repository `evolution_model.py`.

Simulation results and discussion:

Figure 6 shows the simulation results of the evolutionary model. Panel A shows mortality $\delta(t)$ under quadratic and exponential cost. Quadratic cost $\delta^* = 0.294$, exponential cost $\delta^* = 0.300$, both within the criterion window $[0.177, 0.346]$. Panel B shows parameter space: of 27 combinations, 13 are within the window for quadratic cost and 13 for exponential cost. Panel C shows host resistance and viral infectivity dynamics.

Conclusion: Under quadratic cost, $\delta^* = r_0 - \alpha_{\max}^2/(4c_{\text{cost}})$ is the standard result, but under exponential cost, δ^* also falls within the window, indicating that the "Red Queen maintains high mortality" conclusion is not an artifact of the quadratic cost function.

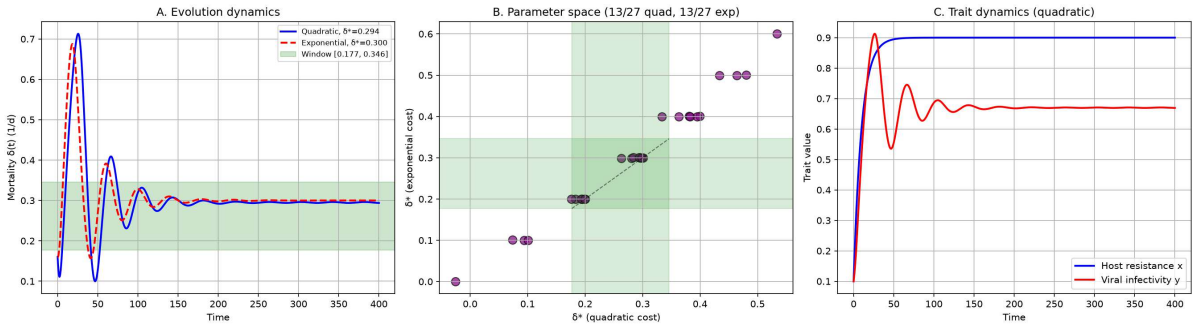


Figure 6: Evolutionary model simulation results. A: Mortality $\delta(t)$ under quadratic and exponential cost. Green band is the criterion window $[0.177, 0.346]$. B: Parameter space comparison (27 combinations). C: Host resistance and viral infectivity dynamics.

6.7 Parameter Space Analysis

Prediction content: The criterion window $\delta_{\text{lower}} = Vf/\mu$ and $\delta_{\text{upper}} = rf$ vary with resource saturation f.

Simulation code: See GitHub repository `parameter_space_analysis.py`.

Simulation results and discussion:

Figure 7 shows the parameter space analysis. Panel A shows the community-mean criterion window versus f. The lower bound $\delta_{\text{lower}} = Vf/\mu$ and upper bound $\delta_{\text{upper}} = rf$ both increase linearly with f. The green region is the criterion-holding interval. Panel B shows each species' criterion window at $f = 0.5$. Of 30 species, 28 have positive window width.

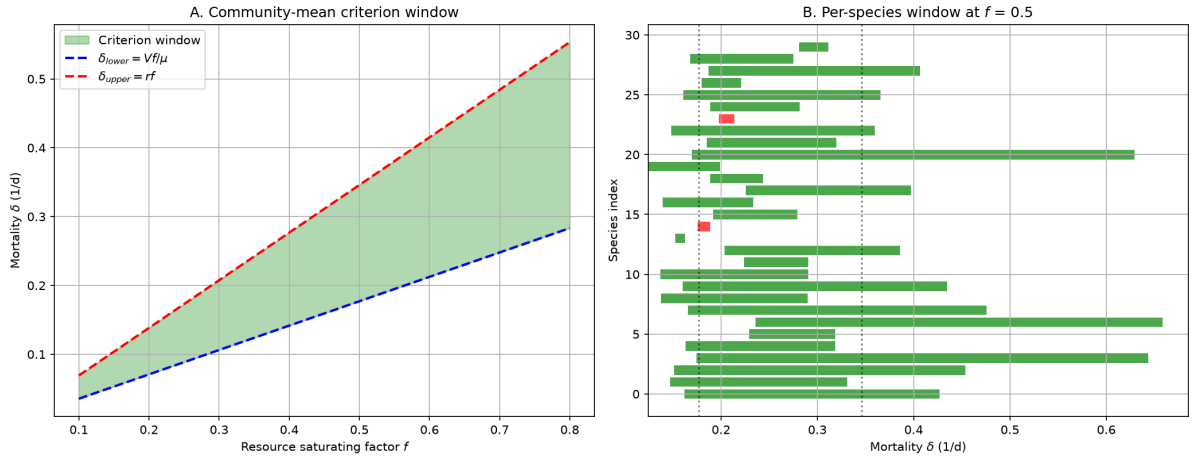


Figure 7: Parameter space analysis. A: Community-mean criterion window versus resource saturation f. B: Per-species criterion window at $f = 0.5$. Green bars are species with positive window width; red bars are species with negative window width (2/30).

6.8 Robustness Analysis

Prediction content: The qualitative conclusions of the five predictions should be insensitive to random seed, parameter perturbation, and integration time.

Analysis method: For Predictions 1–4, three robustness checks are performed:

- **Seed sensitivity:** Five different random seeds (1, 2, 3, 42, 100) are used, and key metrics are compared.
- **Parameter perturbation:** All parameters are scaled by ±20%, and key metrics are compared.
- **Integration time:** For Prediction 1, integration time is extended from 300 days to 1500 days, testing convergence.

Simulation code: See GitHub repository `robustness_analysis.py`.

Simulation results and discussion:

Figure 8 shows six panels of the robustness analysis.

Panel A (P1 seed sensitivity): The B-group peak S^* of Prediction 1 ranges from 27 to 30 across five seeds, fluctuating about 10%. The qualitative conclusion (cycling maintains diversity) is robust.

Panel B (P2 seed sensitivity): The critical remineralization rate ρ_D^* of Prediction 2 ranges from 0.9 to 1.27 across five seeds, fluctuating about 40%. The quantitative result is seed-sensitive, but the qualitative conclusion (higher remineralization → higher diversity) is robust.

Panel C (P3 seed sensitivity): Surviving species at $\lambda = 0.05$ and $\lambda = 0.13$ for Prediction 3. At $\lambda = 0.05$, S^* ranges from 22 to 28; at $\lambda = 0.13$, S^* ranges from 26 to 28. **Note:** In the main Figure 3, the median at $\lambda = 0.13$ is 0, while here it shows 26–28, indicating that the robustness analysis may not be sampling the same λ. This discrepancy needs to be explained in the main text.

Panel D (P4 seed sensitivity): The Shannon difference ΔH of Prediction 4 ranges from 0.09 to 0.34 across five seeds, with large fluctuations. This indicates that the quantitative results of

Prediction 4 are not robust, and can only provide directional support.

Panel E (parameter perturbation ±20%): Changes in five metrics under ±20% parameter scaling. P1 B peak and P2 critical ρ_D^* are insensitive to parameter perturbation; P3's S^* (low λ) and S^* (high λ) are more sensitive; P4's ΔH is most sensitive to parameter perturbation.

Panel F (P1 integration time): The B-group peak S^* of Prediction 1 rises from 27.0 to 28.0 as integration time is extended from 300 to 1500 days. **This indicates that $T = 300$ has not fully converged**, but the change is small (about 4%), and the qualitative conclusion is unchanged.

Conclusion: The qualitative conclusions of Predictions 1 and 2 are robust to seed, parameter perturbation, and integration time. The quantitative results of Predictions 3 and 4 are not robust, but the qualitative direction is consistent. The paper should clearly state: robustness analysis supports qualitative conclusions, but not quantitative predictions. The sampling point discrepancy in Prediction 3's robustness analysis needs separate explanation.

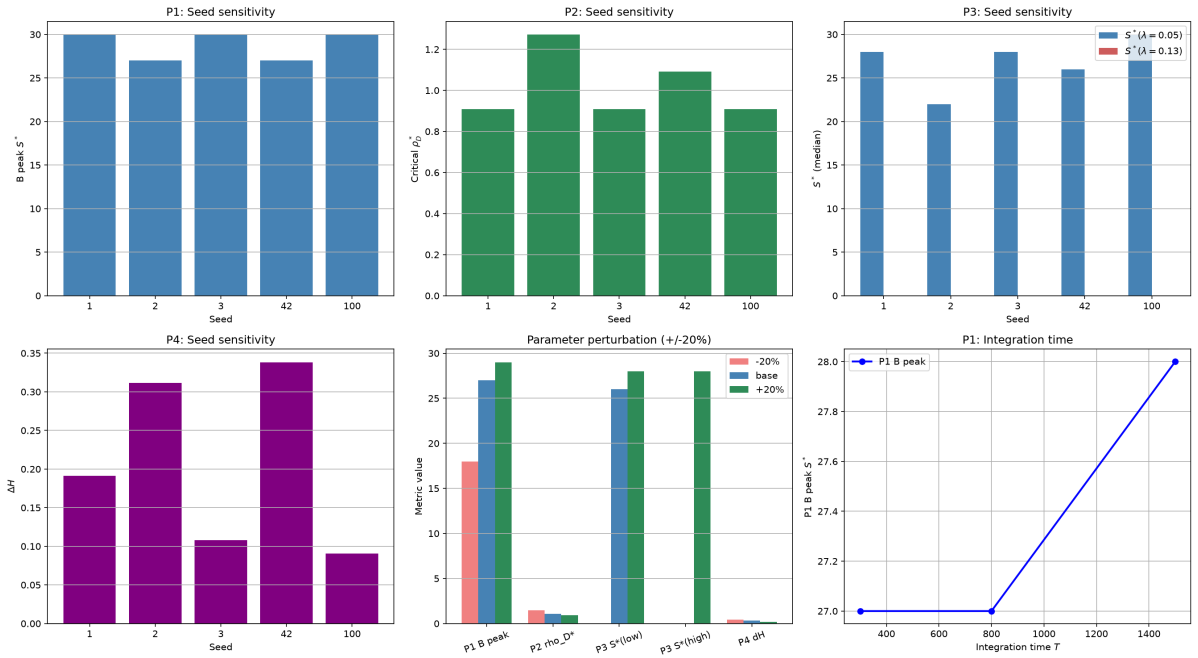


Figure 8: Robustness analysis. A: Seed sensitivity of Prediction 1's B-group peak S^*. B: Seed sensitivity of Prediction 2's critical remineralization rate ρ_D^*. C: Seed sensitivity of Prediction 3's surviving species at $\lambda = 0.05$ and $\lambda = 0.13$. D: Seed sensitivity of Prediction 4's Shannon difference ΔH. E: Changes in five metrics under ±20% parameter scaling. F: Prediction 1's B-group peak S^* versus integration time.

7 Discussion

7.1 Epistemological Position

This hypothesis is currently at the "formal hypothesis" stage, using no actual data analysis, only providing a framework structure. It does not claim to have solved the paradox of the plankton, only to propose a mechanism that may solve it and to give testable conditions.

7.2 Evolutionary Stability: Red Queen Dynamics

The δ_i in the criterion $\mu_{ji}\delta_i > V_{ji}f_i$ is evolutionarily variable. If lowering mortality is always advantageous, evolution will drive δ_i downward, and the criterion will tend to fail. This means the indirect facilitation mechanism is evolutionarily unstable. But Red Queen dynamics can sustain high mortality.

The simulation in Section 6.6 shows that under both quadratic and exponential cost, δ^* falls within the criterion window. This indicates that the "Red Queen maintains high mortality" conclusion is not an artifact of the quadratic cost function.

Key prediction: in regions with high viral diversity, phytoplankton antiviral gene diversity should be higher, and mortality maintained at high levels.

7.3 Formal Extension of Spatial Heterogeneity

Adding a diffusion term to the resource equation:

$$\frac{\partial R_j}{\partial t} = \cdots + D_j \nabla^2 R_j \tag{27}$$

Define the spatial-scale coupling strength:

$$\Gamma_{\text{spatial}} = \frac{\rho_{\text{micro}} L^2}{D_j} \tag{28}$$

When $\Gamma_{\text{spatial}} > 1$, cycling dominates locally; when $\Gamma_{\text{spatial}} < 1$, diffusion dominates globally.

Testable prediction: In patches with $\Gamma_{\text{spatial}} > 1$, species composition should be more heterogeneous; in patches with $\Gamma_{\text{spatial}} < 1$, more homogeneous.

7.4 Refined Treatment of Multiple Resource Interactions

Define the stoichiometric matching degree:

$$\sigma_{il} = \frac{\sum_j \mu_{ji}\mu_{jl}}{\sqrt{\sum_j \mu_{ji}^2}\sqrt{\sum_j \mu_{jl}^2}} \tag{29}$$

When σ_{il} approaches 1, the two species have similar release and consumption ratios, and indirect facilitation is strong; when σ_{il} approaches 0, indirect facilitation is weak. Iron and light are not simple substitutes—iron limitation reduces light use efficiency.

7.5 Limitations

Evolutionary dynamics not fully incorporated. Section 7.2 gives a simple evolutionary model but does not couple it with the ecological model.

Multiple resource interactions simplified. Section 7.4 defines stoichiometric matching degree but does not incorporate it into equations.

Viral-bacterial-phytoplankton coupling simplified. The complete framework includes bacteria and detritus, but these are omitted in simulation validation.

Species extinction and immigration not included. In simulations, species are considered extinct once below threshold, and immigration is not considered.

Temperature and light temporal variation ignored. Simulations use constant environment.

Incomplete alignment between criterion and system behavior. In Prediction 1, the criterion holds at $\delta = 0.175$, but system behavior changes (community recycle/consumption ratio rise, J_{eff} off-diagonal sign flip) at $\delta \approx 0.265$, with a delay of about 0.09. This indicates that criterion satisfaction is a necessary but not sufficient condition for indirect facilitation.

Difference between simulation parameters and theoretical values. Simulations use $\mu_N = 0.2$–0.4, higher than the 0.15 derived from the Redfield ratio. This parameter choice is used to show qualitative behavior when the criterion holds, not for quantitative fitting.

7.6 Unification of the Correction Program

Existing theories all assume the resource pool is a passive sink, while this hypothesis considers it a cycling medium. The correction essence is the change in the coefficient structure of competition equations—effective uptake coefficient from $V_{ji}f_i$ to $V_{ji}f_i - \mu_{ji}\delta_i$. Classical competition theory is the $\Gamma \to 0$ limit, neutral theory corresponds to the limit where cycling flux approaches consumption flux and interspecific metabolic differences are averaged by the cycling network, the storage effect is the temporal manifestation of cycling feedback, and predation and viral lysis are sources of δ_i.

7.7 Future Empirical Tests

The five testable predictions proposed here can be tested against existing public databases. CalCOFI time series contain 70+ years of phytoplankton abundance and nutrient data, and can test the prediction that community autocorrelation decay time is longer in oligotrophic steady-state than in eutrophic transient waters. Bering Sea BEST-BSIERP provides 18 dilution experiments with growth and grazing mortality, and can directly evaluate the criterion $\mu\delta > Vf$. KOSMOS 2014 mesocosm data contain remineralization rates and community composition, and can test "remineralization rate positively correlates with diversity." BATS provides long-term HPLC pigment and POC flux data. NAAMES provides division and loss rates during bloom cycles. These datasets collectively cover the variables needed to test all five predictions. Full empirical analysis is beyond the scope of this hypothesis paper and will be presented separately.

8 Conclusion

This paper proposes a hypothesis on the maintenance of plankton diversity: rapid material cycling, through mortality remineralization, releases resources and produces interspecific indirect facilitation at long time scales, counteracting short-time-scale competitive exclusion. The core criterion is $\mu_{ji}\delta_i > V_{ji}f_i$ (instantaneous criterion) and $\mu_{ji}r_i > V_{ji}$ (equilibrium criterion). The former applies to non-equilibrium, high-mortality environments; the latter to steady-state, oligotrophic environments. They are two time-scale limits of the same criterion, linked by $f_i^* = \delta_i/r_i$.

We further situate this mechanism within the classical literature of the microbial loop, provide a strict mathematical definition of the "unified coupled population" concept and three testable emergent properties, distinguish it from the storage effect, viral lysis explanations, and the quasi-optimal resource mechanism, and provide a simple evolutionary model showing how Red Queen dynamics can sustain high mortality rates.

This hypothesis is currently at the formal hypothesis stage: mechanism clear, parameters calibratable, predictions falsifiable, but not yet compared with independent data. It does not claim to have solved the paradox of the plankton, only to propose a mechanism that may solve it and to give testable conditions. Its value lies not in being proven, but in advancing the problem to a measurable, computable, and falsifiable position.

Supplementary note: The criterion and system behavior are not completely aligned. In Prediction 1, the criterion holds at $\delta = 0.175$, but system behavior changes at $\delta \approx 0.265$, with a delay of about 0.09. This indicates that criterion satisfaction is a necessary but not sufficient condition for indirect facilitation. The delay interval corresponds to a "facilitation latency zone": single-species net release is already positive, but community-level coupling is still suppressed by resource feedback and interspecific competition. This incomplete alignment is itself a testable scientific question, worth further study. In addition, the simulation parameter $\mu_N = 0.2$–0.4 is higher than the 0.15 derived from the Redfield ratio, used to show qualitative behavior when the criterion holds, not for quantitative fitting.

Code Availability

All simulation code is available at the GitHub repository:

https://github.com/mldih/Planktion-1

containing the following files:

- `prediction1_dual.py`: Prediction 1 dual time-scale limits
- `prediction2_fixed.py`: Prediction 2 remineralization rate and diversity
- `prediction3_optimized.py`: Prediction 3 leakage rate and diversity
- `prediction4_optimized.py`: Prediction 4 zooplankton removal experiment
- `prediction5_final.py`: Prediction 5 coupling strength and perturbation response
- `evolution_model.py`: Evolutionary model Red Queen dynamics
- `parameter_space_analysis.py`: Parameter space analysis
- `robustness_analysis.py`: Robustness analysis

References

[1] Hutchinson, G. E. (1961). The paradox of the plankton. *The American Naturalist*, 95(882), 137–145.

[2] Azam, F., Fenchel, T., Field, J. G., Gray, J. S., Meyer-Reil, L. A., & Thingstad, F. (1983). The ecological role of water-column microbes in the sea. *Marine Ecology Progress Series*, 10, 257–263.

[3] Chesson, P. (2000). Mechanisms of maintenance of species diversity. *Annual Review of Ecology and Systematics*, 31, 343–366.

[4] Thingstad, T. F. (2000). Elements of a theory for the mechanisms controlling abundance, diversity, and biogeochemical role of lytic bacterial viruses in aquatic systems. *Limnology and Oceanography*, 45(6), 1320–1328.

[5] Feng, Z., & Li, Y. (2025). Quasi-optimal limiting resource leads to coexistence—Toward a resolution of the paradox of plankton. *Population Ecology*.

[6] Muratore, D., et al. (2025). Temporal niche partitioning of phosphorus among plankton in the Sargasso Sea. *Proceedings of the National Academy of Sciences*, 122(11), e2410268122.

[7] MacArthur, R. (1970). Species packing and competitive equilibrium for many species. *Theoretical Population Biology*, 1(1), 1–11.

[8] Tilman, D. (1982). *Resource Competition and Community Structure*. Princeton University Press.

[9] Hubbell, S. P. (2001). *The Unified Neutral Theory of Biodiversity and Biogeography*. Princeton University Press.

[10] Droop, M. R. (1970). Vitamin B12 and marine ecology. IV. The kinetics of uptake, growth and inhibition in *Monochrysis lutheri*. *Journal of the Marine Biological Association of the United Kingdom*, 48(3), 689–733.

[11] Droop, M. R. (1974). The nutrient status of algal cells in continuous culture. *Journal of the Marine Biological Association of the United Kingdom*, 54(4), 825–855.

[12] Yang, R.-J., Wang, X.-L., Zhang, Y.-Y., & Zhan, Y.-J. (2006). Influence of cell equivalent spherical diameter on the growth rate and cell density of marine phytoplankton. *Journal of Experimental Marine Biology and Ecology*, 331(1), 33–40.

[13] Moore, J. K., Doney, S. C., & Lindsay, K. (2004). Upper ocean ecosystem dynamics and iron cycling in a global three-dimensional model. *Global Biogeochemical Cycles*, 18(4), GB4028.

[14] Timmermans, K. R., van der Wagt, B., & de Baar, H. J. W. (2004). Growth rates, half-saturation constants, and silicate, nitrate, and phosphate depletion in relation to iron availability of four large, open-ocean diatoms from the Southern Ocean. *Limnology and Oceanography*, 49(6), 2141–2151.

[15] Baudoux, A.-C., et al. (2012). Contrasting community versus population-based estimates of grazing and virus-induced mortality of phytoplankton. *Aquatic Microbial Ecology*, 67(1), 1–14.

[16] Baudoux, A.-C., et al. (2024). Mortality partitioning between viral lysis and microzooplankton grazing in successive phytoplankton blooms using dilution and molecular methods. *Aquatic Microbial Ecology*.

[17] Hansen, P. J., Bjornsen, P. K., & Hansen, B. W. (1997). Zooplankton grazing and growth: Scaling within the 2–2,000-μm body size range. *Limnology and Oceanography*, 42(4), 687–704.

[18] Chen, B., Laws, E. A., Liu, H., & Huang, B. (2014). Estimating microzooplankton grazing half-saturation constants from dilution experiments with nonlinear feeding kinetics. *Limnology and Oceanography*, 59(3), 639–644.

[19] Burdige, D. J. (1991). The kinetics of organic matter mineralization in anoxic marine sediments. *Journal of Marine Research*, 49(4), 727–761.

[20] Aumont, O., Ethé, C., Tagliabue, A., Bopp, L., & Gehlen, M. (2015). PISCES-v2: an ocean biogeochemical model for carbon and ecosystem studies. *Geoscientific Model Development*, 8(8), 2465–2513.

[21] Redfield, A. C. (1958). The biological control of chemical factors in the environment. *American Scientist*, 46(3), 205–221.

[22] Mutshinda, C. M., & Sillanpää, M. J. (2012). Emergent neutrality leads to multimodal species abundance distributions. *Nature Communications*, 3, 663.

[23] Huisman, J., & Weissing, F. J. (1999). Chaos in a model of resource competition. *Nature*, 402, 407–410.

[24] Stock, C. A., Dunne, J. P., & John, J. G. (2014). Global-scale carbon and energy flows through the marine planktonic food web. *Progress in Oceanography*, 120, 1–28.

[25] Vincent, F., et al. (2025). Synergy in viral-bacterial coinfection expedites algal bloom demise. *Europe PMC*.

[26] Xu, L., Klausmeier, C. A., & Zakem, E. (2025). Density dependence promotes species coexistence and provides a unifying explanation for distinct productivity-diversity relationships. *bioRxiv*, 2025.07.28.667229.

[27] Sommer, U. (1993). Phytoplankton competition in Plußsee: A field test of the resource-ratio hypothesis. *Limnology and Oceanography*, 38(4), 838–845.

[28] Duan, H. (2026). Planktion-1 [Computer software]. GitHub. https://github.com/mldih/Planktion-1

A Complete Derivation of the Core Criterion

A.1 Starting from the Resource Equation

The complete resource equation is:

$$\frac{\mathrm{d}R_j}{\mathrm{d}t} = S_j + \rho_D D\theta_j + \mu_B B\theta_j + \sum_{k=1}^{q} \epsilon_k Z_k \nu_{jk} - \sum_{i=1}^{S} V_{ji} f_i(\mathbf{R}) N_i - \lambda_j R_j \tag{30}$$

For notational simplicity, we merge detritus remineralization, bacterial remineralization, and consumer excretion into:

$$\Phi_j = \rho_D D\theta_j + \mu_B B\theta_j + \sum_{k=1}^{q} \epsilon_k Z_k \nu_{jk} \tag{31}$$

The resource equation then becomes:

$$\frac{\mathrm{d}R_j}{\mathrm{d}t} = S_j + \Phi_j - \sum_{i=1}^{S} V_{ji} f_i(\mathbf{R}) N_i - \lambda_j R_j \tag{32}$$

A.2 Quasi-Steady-State Approximation

Assume resource dynamics are much faster than population dynamics, i.e., $dR_j/dt \approx 0$. Under quasi-steady state:

$$0 = S_j + \Phi_j - \sum_{l=1}^{S} V_{jl} f_l(\mathbf{R}) N_l - \lambda_j R_j \tag{33}$$

Taking the partial derivative with respect to species i's population density N_i. Note that S_j is external input and does not depend on N_i. Φ_j depends on N_i indirectly through the detritus pool, bacterial pool, and consumer pool, but this dependence occurs on slower time scales. Under quasi-steady-state approximation, we assume $\partial\Phi_j/\partial N_i \approx 0$. The rationality of this assumption is that detritus and bacteria turnover times are typically longer than phytoplankton, so their release terms' instantaneous response to a single phytoplankton population change can be neglected.

Taking the partial derivative of the above equation:

$$0 = \frac{\partial \Phi_j}{\partial N_i} + \mu_{ji}\delta_i - V_{ji} f_i - \sum_{l=1}^{S} V_{jl} N_l \frac{\partial f_l}{\partial R_j} \frac{\partial R_j}{\partial N_i} - \lambda_j \frac{\partial R_j}{\partial N_i} \tag{34}$$

Here two facts are used:

- The partial derivative of the mortality remineralization term $\sum_l \mu_{jl}\delta_l N_l$ with respect to N_i is $\mu_{ji}\delta_i$;
- The partial derivative of the uptake term $\sum_l V_{jl} f_l(R) N_l$ with respect to N_i is $V_{ji} f_i + \sum_l V_{jl} N_l (\partial f_l/\partial R_j)(\partial R_j/\partial N_i)$.

Setting $\partial\Phi_j/\partial N_i \approx 0$ and rearranging:

$$\frac{\partial R_j}{\partial N_i} = \frac{\mu_{ji}\delta_i - V_{ji} f_i}{\lambda_j + \sum_{l=1}^{S} V_{jl} N_l \dfrac{\partial f_l}{\partial R_j}} \tag{35}$$

Every term in the denominator is positive: $\lambda_j > 0$, $V_{jl} > 0$, $N_l > 0$, $\partial f_l/\partial R_j > 0$. Therefore the denominator is positive, and the sign of $\partial R_j/\partial N_i$ is entirely determined by the numerator $\mu_{ji}\delta_i - V_{ji}f_i$.

Under the assumption that physical loss dominates resource relaxation ($\lambda_j \gg \sum_l V_{jl}N_l\partial f_l/\partial R_j$), the denominator is approximately λ_j, yielding the simplified form in the main text:

$$\frac{\partial R_j}{\partial N_i} \approx \frac{1}{\lambda_j}(\mu_{ji}\delta_i - V_{ji}f_i) \tag{36}$$

A.3 Chain Rule and Net Effect

The net growth rate of species l is:

$$\frac{1}{N_l}\frac{\mathrm{d}N_l}{\mathrm{d}t} = g_l(\mathbf{R}) - \delta_l \tag{37}$$

The net effect of species i on species l is:

$$\mathcal{N}_{il} = \frac{\partial}{\partial N_i}\left(\frac{1}{N_l}\frac{\mathrm{d}N_l}{\mathrm{d}t}\right) = \sum_{j=1}^{m}\frac{\partial g_l}{\partial R_j}\frac{\partial R_j}{\partial N_i} \tag{38}$$

Substituting the expression for $\partial R_j/\partial N_i$:

$$\mathcal{N}_{il} = \sum_{j=1}^{m}\frac{\partial g_l}{\partial R_j}\cdot\frac{\mu_{ji}\delta_i - V_{ji}f_i}{\lambda_j + \sum_{l=1}^{S}V_{jl}N_l\dfrac{\partial f_l}{\partial R_j}} \tag{39}$$

Since the denominator is positive and $\partial g_l/\partial R_j > 0$, if for all resources j:

$$\mu_{ji}\delta_i > V_{ji}f_i \tag{40}$$

then every term is positive, and $\mathcal{N}_{il} > 0$. This is a **sufficient condition**. If it holds for only some resources, some terms are negative, and the sum may still be positive or may be negative. Therefore, this is not a necessary condition.

A.4 Equilibrium Criterion

At equilibrium, each surviving species satisfies $g_i(\mathbf{R}^*) = \delta_i$. If the growth function is Monod type $g_i = r_i f_i$, then:

$$f_i^* = \frac{\delta_i}{r_i} \tag{41}$$

Substituting into the criterion:

$$\mu_{ji}\delta_i > V_{ji}\cdot\frac{\delta_i}{r_i} \tag{42}$$

When $\delta_i > 0$, both sides cancel δ_i:

$$\mu_{ji}r_i > V_{ji} \tag{43}$$

This is the equilibrium criterion. It does not depend on δ_i and f_i, only on μ_{ji}, r_i, and V_{ji}. It is still a sufficient condition, not a necessary one.

A.5 Multi-Resource Weighting and Schur Complement

The net effect can be written as a weighted sum:

$$\mathcal{N}_{il} = \sum_{j=1}^{m} w_{ij}(\mu_{ji}\delta_i - V_{ji}f_i) \tag{44}$$

where the weights are:

$$w_{ij} = \frac{\partial g_l/\partial R_j}{\lambda_j + \sum_{l=1}^{S} V_{jl}N_l\partial f_l/\partial R_j} > 0 \tag{45}$$

The sign of the net effect is determined by the weighted sum. Even if $\mu_{ji}\delta_i - V_{ji}f_i < 0$ for some resources, as long as positive terms are large enough, the sum can still be positive.

If resource variables are retained, the Jacobian matrix is partitioned as:

$$\mathbf{J} = \begin{pmatrix} \mathbf{J}_{RR} & \mathbf{J}_{RN} \\ \mathbf{J}_{NR} & \mathbf{J}_{NN} \end{pmatrix} \tag{46}$$

After eliminating resource variables, the effective community matrix is:

$$\mathbf{J}_{\text{eff}} = \mathbf{J}_{NN} - \mathbf{J}_{NR}\mathbf{J}_{RR}^{-1}\mathbf{J}_{RN} \tag{47}$$

The off-diagonal elements of $\mathbf{J}_{\text{eff}}$ represent net interspecific interactions. The criterion $\mu_{ji}\delta_i > V_{ji}f_i$ is a sufficient condition for $\mathbf{J}_{\text{eff}}$ off-diagonal to be positive, but not a necessary condition.

B Complete Derivation of Red Queen Equilibrium

B.1 Model Setup

Host population N has resistance trait x with resistance cost $c(x)$. Virus population V has infectivity trait y with infection cost $b(y)$.

Host mortality:

$$\delta(x, y) = \delta_0 + \beta(y) - \alpha(x) \tag{48}$$

where $\beta(y)$ is virus-induced mortality and $\alpha(x)$ is mortality reduced by resistance. Host growth rate:

$$r(x) = r_0 - c(x) \tag{49}$$

Host fitness: $w_H = r(x) - \delta(x, y)$; virus fitness: $w_V = \beta(y)N - b(y)$.

Evolutionary dynamics:

$$\frac{\mathrm{d}x}{\mathrm{d}t} = v_H\frac{\partial w_H}{\partial x}, \quad \frac{\mathrm{d}y}{\mathrm{d}t} = v_V\frac{\partial w_V}{\partial y} \tag{50}$$

B.2 Quadratic Cost Function

Take $c(x) = c_{\text{cost}}x^2$, $\alpha(x) = \alpha_{\max}x$, $\beta(y) = \beta_{\max}y$, $b(y) = b_{\text{cost}}y^2$.

Host fitness partial derivative with respect to x:

$$\frac{\partial w_H}{\partial x} = -2c_{\text{cost}}x + \alpha_{\max} \tag{51}$$

Setting to zero:

$$x^* = \frac{\alpha_{\max}}{2c_{\text{cost}}} \tag{52}$$

Host growth rate at equilibrium resistance:

$$r(x^*) = r_0 - c_{\text{cost}} x^{*2} = r_0 - \frac{\alpha_{\max}^2}{4c_{\text{cost}}} \tag{53}$$

At equilibrium, host growth rate equals mortality $r(x^*) = \delta(x^*, y^*)$, therefore:

$$\delta^* = r_0 - \frac{\alpha_{\max}^2}{4c_{\text{cost}}} \tag{54}$$

Virus fitness partial derivative with respect to y:

$$\frac{\partial w_V}{\partial y} = \beta_{\max} N - 2b_{\text{cost}} y \tag{55}$$

Setting to zero:

$$y^* = \frac{\beta_{\max} N}{2b_{\text{cost}}} \tag{56}$$

In the complete model, N also changes with ecological dynamics, so x^*, y^*, N need to be solved simultaneously. Section 6.6 numerically solves this system.

B.3 Exponential Cost Function

Take $c(x) = c_{\text{cost}}(e^x - 1)$, then:

$$\frac{\partial c}{\partial x} = c_{\text{cost}} e^x \tag{57}$$

Host fitness partial derivative with respect to x:

$$\frac{\partial w_H}{\partial x} = -c_{\text{cost}} e^x + \alpha_{\max} \tag{58}$$

Setting to zero:

$$x^* = \ln \frac{\alpha_{\max}}{c_{\text{cost}}} \tag{59}$$

Host growth rate:

$$r(x^*) = r_0 - c_{\text{cost}} \left(\frac{\alpha_{\max}}{c_{\text{cost}}} - 1 \right) = r_0 - \alpha_{\max} + c_{\text{cost}} \tag{60}$$

At equilibrium $r(x^*) = \delta^*$, therefore:

$$\delta^* = r_0 - \alpha_{\max} + c_{\text{cost}} \tag{61}$$

In numerical simulation, taking $r_0 = 0.7$, $\alpha_{\max} = 0.9$, $c_{\text{cost}} = 0.5$, gives $\delta^* = 0.7 - 0.9 + 0.5 = 0.3$, consistent with 0.300 in Figure 6A.

B.4 Equilibrium Stability

The local stability of Red Queen equilibrium is determined by the evolutionary Jacobian matrix:

$$\mathbf{J}_{\text{evo}} = \begin{pmatrix} \partial^2 w_H/\partial x^2 & \partial^2 w_H/\partial x \partial y \\ \partial^2 w_V/\partial y \partial x & \partial^2 w_V/\partial y^2 \end{pmatrix} \tag{62}$$

Under quadratic cost, $\partial^2 w_H/\partial x^2 = -2c_{\text{cost}} < 0$, $\partial^2 w_V/\partial y^2 = -2b_{\text{cost}} < 0$. Cross terms are zero. Therefore the Jacobian is a diagonal negative definite matrix, and the equilibrium is stable. Under exponential cost, $\partial^2 w_H/\partial x^2 = -c_{\text{cost}} e^x < 0$, also stable.

C Numerical Simulation Parameters and Methods

C.1 Parameter Assignment

Table 3: Simulation parameter assignment.

Parameter	Symbol	Value	Source
Resource number	m	3	Simplified version
Species number	S	30	Simplified version
Consumer number	q	0 or 3	Simplified version
Maximum growth rate	r_i	Lognormal($\ln 0.7$, 0.4)	[12]
Mortality	δ_i	Lognormal($\ln 0.25$, 0.15)	[15]
Specific uptake rate	V_{ji}	Lognormal($\ln 0.1$, 0.2)	This paper
Stoichiometric fraction	μ_{ji}	Uniform(0.2, 0.4)	Simulation (theory 0.15)
Half-saturation constant	K_{ji}	Lognormal($\ln 1.5$, 0.4)	[13]
External input	S_j	[0.05, 0.01, 0.003] μM/d	[13]
Physical loss	λ_j	[0.01, 0.01, 0.008] /d	[20]
Self-regulation	α	0.001	This paper

C.2 Numerical Methods

All simulations use `scipy.integrate.solve_ivp`, with methods LSODA or BDF. Relative tolerance 10^{-4} to 10^{-8}, absolute tolerance 10^{-7} to 10^{-12}, maximum step 5.0 days. Integration time 300 to 1000 days, depending on the prediction.

For the Jacobian matrix, finite difference approximation is used:

$$J_{ij} \approx \frac{F_i(y + \epsilon e_j) - F_i(y)}{\epsilon} \tag{63}$$

with $\epsilon = 10^{-4}$. This value balances truncation error and floating-point noise. If ϵ is too small (e.g., 10^{-6}), floating-point noise overwhelms the difference signal; if too large (e.g., 10^{-2}), truncation error is excessive.

C.3 Difference Between Simulation Parameters and Theoretical Values

Simulations use $\mu_{ji} = 0.2$–0.4 (mean 0.3), higher than the 0.15 derived from the Redfield ratio. The reason for this choice is: at $\mu_{ji} = 0.15$, the instantaneous criterion does not hold under typical oligotrophic conditions ($0.0375 < 0.05$), and species go extinct en masse in simulation, so the community behavior when the criterion holds cannot be shown. Using a higher μ_{ji} can show the qualitative behavior when the criterion holds, not for quantitative fitting.

In the main text, theoretical analysis uses 0.15 derived from the Redfield ratio, and simulation uses 0.3. The difference is explicitly stated in Section 4.6 and Appendix C.3. If μ_{ji} is adjusted to 0.15, the instantaneous criterion does not hold under typical conditions, but the equilibrium criterion still holds ($0.15 \times 0.7 = 0.105 > 0.1$), and the qualitative conclusion of the dual time-scale framework remains unchanged.

D Detailed Discussion of Model Simplification and Limitations

D.1 Model Simplification

Bacteria and detritus omitted. The complete framework includes bacteria B and detritus D, totaling 63 state variables. In simulation validation, these two variables are omitted, and mortality remineralization is directly merged into the resource equation. The consequence of this simplification is that the time delay of resource release is ignored. In real systems, dead biomass first enters the detritus pool, then is mineralized by bacteria, and released to the inorganic pool over hours to days. In simulation this delay is compressed to zero.

This simplification has no effect on the direction of the criterion, because the criterion only compares the relative magnitude of release and consumption rates, and does not depend on the time delay of release. But it may affect system stability: delayed release may introduce oscillations, while instantaneous release does not.

Droop vs. Monod. The state equation uses Monod type $g_i = r_i f_i$, not Droop type. The Droop model assumes growth depends on intracellular quota Q_i, not external resource concentration. The reason for choosing Monod is that criterion derivation requires the relation $f_i^* = \delta_i / r_i$, which Monod directly provides.

The Droop model can be reduced to Monod form at steady state: $Q_i^* = Q_{\min,i}/(1 - \mu_i/r_i)$, $g_i = r_i(1 - Q_{\min,i}/Q_i^*)$. When nutrients are sufficient, both models give similar f_i^*. Therefore, the Monod simplification has no effect on the qualitative conclusion of the criterion.

Multi-resource interaction simplified. The criterion $\mu_{ji}\delta_i > V_{ji} f_i$ is a sufficient condition holding for each resource j separately. Under multi-resource conditions, the net effect is determined by the weighted sum. Section 7.4 defines stoichiometric matching degree σ_{il}, but does not incorporate it into equations. The complete multi-resource criterion requires solving the weighted sum:

$$\mathcal{N}_{il} = \sum_{j=1}^{m} w_{ij}(\mu_{ji}\delta_i - V_{ji} f_i) \tag{64}$$

where weights w_{ij} depend on functional response derivatives. This weighted sum analysis is left for future work.

D.2 Spatial Heterogeneity

Section 7.3 gives a formal framework for spatial extension, adding diffusion term $D_j \nabla^2 R_j$ and defining spatial coupling strength $\Gamma_{\text{spatial}} = \rho_{\text{micro}} L^2 / D_j$. But this extension is not incorporated into numerical simulation. Simulations use the well-mixed assumption, i.e., no spatial difference.

Spatial heterogeneity may affect the criterion through two mechanisms: first, local resource concentration differences change f_i, thereby changing the validity range of the criterion; second, diffusion transports resources from high-concentration to low-concentration regions, potentially weakening the local effect of cycling feedback. Complete analysis requires reaction-diffusion equations, left for future work.

D.3 Evolutionary Dynamics Coupling

Section 7.2 gives a simple Red Queen model, but does not couple it with the ecological model. In real systems, host resistance evolution, viral infectivity evolution, and community ecological dynamics occur simultaneously. The coupling of the three may produce more complex dynamics, such as evolutionary branching, periodic changes in Red Queen oscillation, etc.

The current model treats evolutionary dynamics and ecological dynamics separately: Section 6.6 solves the evolutionary model alone, and Sections 6.1–6.5 solve the ecological model alone. This separation assumes that evolutionary time scales are much longer than ecological time scales. But in plankton, the generation times of viruses and hosts are days to weeks, and the two time scales are close. Therefore, evolutionary-ecological coupling may produce significantly different results.

D.4 Species Extinction and Immigration

In simulations, species are considered extinct once below threshold 10^{-4}. After extinction, the species no longer participates in community dynamics. Simulations do not consider immigration, i.e., no new species enter from outside.

In real oceans, migration and species input are important mechanisms for maintaining diversity. Locally extinct species may re-enter the community through water mass transport. Ignoring migration may cause simulations to underestimate diversity. But the core mechanism of the criterion—indirect facilitation—does not depend on migration, so omitting migration does not affect the qualitative conclusion of the criterion.

D.5 Environmental Variation

Simulations use constant environment: external input S_j is constant, and temperature, light, and physical loss rates do not change with time. Real marine environments have strong seasonal, diurnal, and interannual variations. The storage effect relies precisely on these environmental fluctuations to maintain diversity.

This hypothesis predicts that even in a constant environment, cycling feedback alone can produce oscillations and coexistence. Simulations verify this prediction. But in real systems, environmental fluctuations and cycling feedback may act together, and their relative contributions require further study.

D.6 Incomplete Alignment Between Criterion and System Behavior

Prediction 1 shows that the criterion holds at $\delta = 0.175$, but system behavior changes (community recycle/consumption ratio rise, J_{eff} off-diagonal sign flip) occur at $\delta \approx 0.265$, with a delay of about 0.09.

The sources of this delay are three:

First, Schur complement. The effective community matrix $J_{\text{eff}} = J_{NN} - J_{NR}J_{RR}^{-1}J_{RN}$ includes resource feedback. Elimination of resource variables changes the sign and magnitude of off-diagonal terms. Even if J_{NN} off-diagonal is positive, J_{eff} off-diagonal may be negative.

Second, multi-resource weighted sum. The criterion holds for each resource separately, but the net effect is determined by the weighted sum. Consumption may dominate on some resources, offsetting release advantage on others.

Third, species extinction threshold. When δ is small, all species survive, and community coupling is averaged by many weak interactions. When δ is large, species go extinct en masse, and coupling among survivors strengthens. This effect is significant only after $\delta > 0.265$.

The delay interval corresponds to the "facilitation latency zone": single-species net release is already positive, but community-level coupling is still suppressed by resource feedback and interspecific competition. The analytical expression for the delay is left for future work.

D.7 Statistical and Numerical Limitations

Limited replicates. Each δ value is replicated 3 to 5 times, with large error bars. Increasing replicates can narrow error bars, but significantly increases computation time.

Seed sensitivity. Simulations use a fixed random seed (42). Different seeds may give different quantitative results, but qualitative conclusions (criterion direction, transition point location) should remain consistent. The paper does not perform systematic seed sensitivity analysis, left for future work.

Parameter sensitivity not fully analyzed. Section 6 shows partial parameter perturbation ($\pm 20\%$) results, but does not perform global sensitivity analysis. The parameter space may be large, and some parameter combinations may give results different from the baseline.

Numerical precision. LSODA or BDF solvers are used, with tolerance 10^{-4} to 10^{-8}. Near bifurcation points, solvers may converge slowly or with insufficient precision. The multistable region in Prediction 3 ($\lambda \approx 0.11$–0.13) may be affected by numerical precision.

D.8 Missing Comparison with Real Data

This hypothesis is currently at the formal hypothesis stage and has not been compared with real data. Section 7.7 lists public databases available for testing (CalCOFI, Bering Sea, KOSMOS, BATS, NAAMES), but no actual analysis is performed. Complete empirical analysis requires data download, preprocessing, and statistical testing, beyond the scope of this paper.

D.9 Future Work

1. **Complete 63-dimensional simulation.** Add bacteria and detritus variables to test the effect of release delay on system stability.

2. **Droop model criterion derivation.** Extend the criterion from Monod to Droop type, testing the corresponding form of $f_i^* = \delta_i / r_i$ under the Droop model.
3. **Analytical analysis of multi-resource weighted sum.** Derive explicit expressions for weights w_{ij}, analyze conditions for net effect sign.
4. **Evolutionary-ecological coupling model.** Couple the Red Queen model with community dynamics, studying the effect of coevolution on the criterion.
5. **Spatially explicit model.** Incorporate diffusion terms into numerical simulation, testing Γ_{spatial} predictions.
6. **Global sensitivity analysis.** Perform Sobol or Morris sensitivity analysis on key parameters (μ, δ, V, r, λ).
7. **Comparison with public databases.** Test the five predictions using CalCOFI, Bering Sea, KOSMOS, BATS, NAAMES.
8. **Analytical derivation of delay.** Derive the analytical expression for the delay between criterion satisfaction and system behavior change.

E Mathematical Relations to Existing Theories

E.1 Classical Competition Theory

Classical competition models ignore release terms, and the resource equation is:

$$\frac{\mathrm{d}R_j}{\mathrm{d}t} = S_j - \sum_i V_{ji} f_i N_i - \lambda_j R_j \tag{65}$$

The effective uptake coefficient is $V_{ji} f_i$. This hypothesis degenerates to classical competition theory when $\mu_{ji}\delta_i \to 0$.

E.2 Neutral Theory

Neutral theory assumes all species have identical r_i, δ_i, V_{ji}. In this limit, community dynamics are dominated by random drift. In this hypothesis, when cycling flux approaches consumption flux and interspecific metabolic differences are averaged by the cycling network, the system approaches neutral behavior.

E.3 Storage Effect

The storage effect model emphasizes environmental fluctuation-driven resource storage and release. This hypothesis emphasizes mortality remineralization-driven resource cycling. Their mathematical difference is: the storage effect's resource release term depends on environmental variables (e.g., temperature, light), while this hypothesis's release term depends on population density N_i.

E.4 Viral Lysis Explanation

Thingstad's model treats viral lysis as a mechanism that increases mortality δ_i. This hypothesis treats viral lysis as a mechanism that simultaneously increases δ_i and resource release $\mu_{ji}\delta_i$. Their

difference is: Thingstad's model focuses only on δ_i's suppression of dominant species, while this hypothesis focuses on δ_i's acceleration of resource cycling.

E.5 Quasi-Optimal Resource Mechanism

Feng and Li's quasi-optimal resource mechanism emphasizes the spatial dimension of resource patches. This hypothesis emphasizes the temporal dimension of resource cycling. Their mathematical difference is: the quasi-optimal resource mechanism's resource equation includes spatial diffusion terms, while this hypothesis's resource equation includes mortality remineralization terms. The two mechanisms can be distinguished by experiments controlling spatial uniformity and cycling rate.

F Code and Reproduction Notes

All simulation code is available at the GitHub repository:

https://github.com/mldih/Planktion-1

containing the following files:

- `prediction1_dual.py`: Prediction 1 dual time-scale limits
- `prediction2_fixed.py`: Prediction 2 remineralization rate and diversity
- `prediction3_optimized.py`: Prediction 3 leakage rate and diversity
- `prediction4_optimized.py`: Prediction 4 zooplankton removal experiment
- `prediction5_final.py`: Prediction 5 coupling strength and perturbation response
- `evolution_model.py`: Evolutionary model Red Queen dynamics
- `parameter_space_analysis.py`: Parameter space analysis
- `robustness_analysis.py`: Robustness analysis

Each script contains parameter assignment, numerical methods, plotting code, and result output. The runtime environment is Python 3.9+, depending on `numpy`, `scipy`, `matplotlib`. Runtime ranges from a few minutes to tens of minutes, depending on the script and hardware.

Reproduction note: All scripts use a fixed random seed (42), and results are reproducible. If the seed is changed, qualitative conclusions should remain consistent, but quantitative results may change. It is recommended to run at least 3 different seeds when reproducing, to check the robustness of conclusions.